



## OPEN ACCESS

## EDITED BY

Harsh Mathur,  
Teagasc Food Research Centre, Teagasc,  
Ireland

## REVIEWED BY

Pinkuan Zhu,  
East China Normal University, China  
Duc-Cuong Bui,  
University of Texas Medical Branch at  
Galveston, United States  
Ang Ren,  
Nanjing Agricultural University,  
China

## \*CORRESPONDENCE

Dan Shu  
✉ shudan@cib.ac.cn  
Hong Tan  
✉ abath@cib.ac.cn

## SPECIALTY SECTION

This article was submitted to  
Microbial Physiology and Metabolism,  
a section of the journal  
Frontiers in Microbiology

RECEIVED 31 October 2022

ACCEPTED 23 December 2022

PUBLISHED 26 January 2023

## CITATION

Chen D, Shu D, Wei Z, Luo D, Yang J,  
Li Z and Tan H (2023) Combined  
transcriptome and proteome analysis of  
Bcfrp1 involved in regulating the  
biosynthesis of abscisic acid and growth in  
*Botrytis cinerea* TB-31.  
*Front. Microbiol.* 13:1085000.  
doi: 10.3389/fmicb.2022.1085000

## COPYRIGHT

© 2023 Chen, Shu, Wei, Luo, Yang, Li and  
Tan. This is an open-access article  
distributed under the terms of the [Creative  
Commons Attribution License \(CC BY\)](https://creativecommons.org/licenses/by/4.0/). The  
use, distribution or reproduction in other  
forums is permitted, provided the original  
author(s) and the copyright owner(s) are  
credited and that the original publication in  
this journal is cited, in accordance with  
accepted academic practice. No use,  
distribution or reproduction is permitted  
which does not comply with these terms.

# Combined transcriptome and proteome analysis of Bcfrp1 involved in regulating the biosynthesis of abscisic acid and growth in *Botrytis cinerea* TB-31

Dongbo Chen<sup>1,2</sup>, Dan Shu<sup>1\*</sup>, Zhao Wei<sup>1,2</sup>, Di Luo<sup>1</sup>, Jie Yang<sup>1</sup>,  
Zheming Li<sup>1</sup> and Hong Tan<sup>1\*</sup>

<sup>1</sup>CAS Key Laboratory of Environmental and Applied Microbiology, Environmental Microbiology Key Laboratory of Sichuan Province, Chengdu Institute of Biology, Chinese Academy of Sciences, Chengdu, China, <sup>2</sup>Chengdu Institute of Biology, China Academy of Sciences (CAS), University of the Chinese Academy of Sciences, Chengdu, China

**Introduction:** Abscisic acid (ABA) is an important sesquiterpene compound that regulates the stress resistance of plants. *Botrytis cinerea* can synthesize ABA via the mevalonic acid pathway. To identify the functional genes that are involved in the biosynthesis of ABA, we performed insertion mutagenesis into *B. cinerea* TB-31.

**Methods:** We obtained the ABA-reduced mutant E154 by insertion mutagenesis, and we identified the insertion site was located upstream of the gene *bcrp1* by Thermal asymmetric interlaced PCR. We performed a detailed phenotypic characterization of the *bcrp1* knockout and complementation mutants in TB-31. Furthermore, transcriptome and proteome analyses were conducted to explore how *bcrp1* affects the level of the ABA biosynthesis.

**Results:** The *bcrp1* gene encodes an F-box protein. The phenotypic results confirmed the positive contribution of *bcrp1* to the biosynthesis of ABA and growth. Between TB-31 and  $\Delta$ Bcfrp1, we obtained 4,128 and 1,073 differentially expressed genes and proteins, respectively. The impaired ABA biosynthesis in the  $\Delta$ Bcfrp1 mutants was primarily affected by the different levels of expression of the ABA biosynthetic gene cluster and the genes involved in the mevalonic acid pathway. In addition, we further characterized the differentially expressed genes and proteins that participated in the growth, secondary metabolism, and signal transduction in *B. cinerea* based on the transcriptome and proteome data.

**Discussion:** This research based on the transcriptome and proteome analyses to display the changes after the deletion of *bcrp1* in *B. cinerea* TB-31, will help us to explore the molecular mechanism of ABA biosynthesis in *B. cinerea*.

## KEYWORDS

*bcrp1*, *Botrytis cinerea*, abscisic acid, carbon metabolism, transcriptome, proteome

## 1. Introduction

Abscisic acid (ABA) is a sesquiterpene “stress hormone,” which has been shown to be synthesized not only in plants, but also in cyanobacteria, fungi, sponge, human cells amongst others (Gill and Patranabis, 2021). The most common functions of ABA are involved in controlling seed maturation and germination, increasing the tolerance of plants for various kinds of stresses caused by abiotic or biotic factors (Alazem and Lin, 2017). In addition, ABA has also demonstrated its important functions in other organisms (Sakthivel et al., 2016). It plays important roles in regulating the activation of innate immune cells and glucose homeostasis in mammals (Gietler et al., 2020). Interestingly ABA also seems to exist as a communication signal between different species (Lievens et al., 2017). There are reports of some mutualistic host-microbe and host-pathogen interactions dependence on ABA (Lievens et al., 2017; Hewage et al., 2020). For these reasons, it is very important to understand the biosynthesis and regulation mechanism of ABA in non-plant organisms. It will be very interesting to elucidate the biological significant of ABA as a ‘universal molecule’.

Phytopathogenic fungi, such as *Botrytis cinerea* has been shown to produce ABA. Marumo et al., first reported that the gray mold fungus *B. cinerea* could synthesize ABA in 1982 (Marumo et al., 1982). After that, other *B. cinerea* strains have been confirmed and considered to be ABA-producing strains (De Simone et al., 2020). Twenty years ago, our research group isolated a wild type strain *Botrytis cinerea* TBC-6 from the stems and leaves of wheat in southwest China. Mutant strains TB-31 (with ABA productivity of 0.55 g/L) and TB-3-H8 (with an ABA productivity of 1.4 g/L) were generated after multiple rounds of mutagenesis and screening of TBC-6 (Gong et al., 2014; Wang et al., 2018). Further strain improvement generated the TBC-A strain with an ABA productivity of 2.0 g/L, which has been utilized to reduce the cost of ABA in industrial applications (Gong et al., 2014; Ding et al., 2015). However, little is known about in the molecular mechanisms underlying fungal ABA biosynthesis before these strains can be used in an industrial setting for biotechnological ABA production (Ding et al., 2016).

<sup>18</sup>O-, <sup>2</sup>H-, and <sup>13</sup>C-labeling experiments were performed to study the ABA biosynthetic pathway of *B. cinerea*, and a pathway different from plants has been postulated: isopentenyl pyrophosphate (IPP), which is synthesized from the mevalonic acid (MVA) pathway, is converted to C<sub>15</sub> compound farnesyl diphosphate (FPP). Additionally, after a series of reactions of cyclization, isomerization, desaturation and hydroxylation from FPP, ABA is synthesized (Nambara and Marion-Poll, 2005; Siewers et al., 2006). But there was no genetic information to support this hypothesis, and it was not until 2004 that genes involved in ABA synthesis were discovered. The gene knockout experiments revealed the *bcaba1-4* gene cluster, in which *bcaba1*, 2, 4 genes were presumed to be responsible for the hydroxylation of carbon atoms C-4', C-1' and the oxidation of C-4' of ABA in *B. cinerea*, respectively (Siewers et al., 2004, 2006).

In order to further understand the synthesis and regulatory mechanisms of ABA, we had carried out systematic research in the previous work. First, Ding et al. (2016) performed a comparative transcriptome analysis to identify the differentially expressed genes which may potentially contribute to the very different phenotypic outcomes of ABA production of the industrial strain TBC-A and the wild-type strain TBC-6. The results of comparative transcriptome analysis helps us understand the crucial genes and metabolic pathways related to ABA biosynthesis, including genes involved in the MVA pathway and the biosynthesis of FPP, which further confirmed that the ABA synthesis pathway of fungi is different from that of plants (Ding et al., 2016). Second, the genes that are required for ABA production and regulation were identified based on the transcriptome data, such as *bcaba3*, *bcabaR1*, and *bclaeA*. In our previous study, the targeted disruption of *Bcaba3* showed the loss of ABA synthesis in TB-31, and enabled the detection of 2Z,4E- $\alpha$ -ionylideneethane (data not published). Shu et al. (2018) found that *Bcaba3* can catalyze the substrate FPP into 2Z,4E- $\alpha$ -ionylideneethane through the enzyme catalysis experiments, which is consistent with the report of Takino et al. (2018). Wang et al. (2018) reported a Cys<sub>2</sub>His<sub>2</sub> Zinc finger transcription factor *BcabaR1* which positively regulates the levels of transcription of *bcaba1-4*, by interacting with conserved sequence regions of the ABA gene clusters promoters. Wei et al. (2022) found the global regulator *BcLaeA*, as ‘a putative methyltransferase’, also participates in regulating the biosynthesis of ABA in TB-31 (Wei et al., 2022). Third, in order to find some new unknown genes that may be involved in ABA synthesis, we also performed insertional mutagenesis in *B. cinerea* TB-31 by *Agrobacterium tumefaciens*-mediated transformation (ATMT; Chen et al., 2011), which is a useful approach that enables the identification of functional genes.

Plasmid insertion induction is a common method for identifying new genes or discovering new functions of the known gene (Miesel et al., 2003). Duyvesteijn et al. (2005) obtained a pathogenic deletion mutant from *Fusarium oxysporum* f. sp. *lycopersici* by random insertion, and identified that the insertion site occurred in a gene encoding an F-box protein and named *Frp1* (Duyvesteijn et al., 2005). It was reported that F-box protein (FBP) is part of SCFs (Skp1-cullin-F-box protein ligase) complexes and linked to the Skp1 protein through the F-box (Gabriel et al., 2021). Of course, F-box proteins function as non-SCF complexes, too (Sadat et al., 2021; Wu et al., 2022). Each eukaryote contains a considerable amount of F-box proteins, and each protein may correspond to a substrate. Lots of fungal F-box protein were revealed, which have been shown to be involved in stress response, catabolite repression, and to be a novel virulence factor that shapes immunogenicity and such (De Assis et al., 2018; Masso-Silva et al., 2018; Sharma et al., 2021). However, there are few reports about the effects of F-box protein on secondary metabolic synthesis in fungi.

In this research, we report an ABA deficient mutant *B. cinerea* E154 from an ATMT-mediated random mutation, and the F-box protein *Bcfrp1* was identified which was responsible for the

phenotype of E154. It has not been reported that ubiquitin-related proteins are involved in the regulation of ABA synthesis in *B. cinerea*. The role of *Bcfrp1* in ABA biosynthesis and the growth of *B. cinerea* was investigated. A stringent comparative transcriptome and proteome analysis was performed to identify differentially expressed genes participating in the metabolic pathways related to ABA biosynthesis and other pathways in *B. cinerea*. This study could help us to predict and screen genes related to the effect of *bctrp1* on ABA biosynthesis in *B. cinerea* based on the transcriptome and proteome.

## 2. Materials and methods

### 2.1. Strains, plasmids, and culture conditions

*Escherichia coli* DH5 $\alpha$  and *Agrobacterium tumefaciens* EHA105 were used to construct vectors and transform plasmid DNA. *E. coli* and *A. tumefaciens* strains were grown on Luria-Bertani (LB) media. The plasmid pBHT2 enables the selection of hygromycin-resistant (*hph*) transformants. The ABA-producing strain *B. cinerea* TB-31 was transformed with pBHT2 to create insertional mutants by ATMT (Rolland et al., 2003). *B. cinerea* TB-31 was used as a control for this study to generate gene knockout and complementary mutants of *bctrp1*. *B. cinerea* strains grow on potato glucose agar (PDA) media at 26°C for 7 days, followed by the collection of spores and resuspended to  $1 \times 10^6$  conidia·mL<sup>-1</sup>. The PDA plates with 50  $\mu$ g·mL<sup>-1</sup> hygromycin B or 100  $\mu$ g·mL<sup>-1</sup> glufosinate-ammonium, were purchased from Solar Biotech, to screen the *B. cinerea* transformants.

### 2.2. Construction of the deletion and complementation mutants of *bctrp1*

We generated knockout and complementary mutants of *bctrp1* to explore whether this gene affected the synthesis of ABA in *B. cinerea* TB-31. Lists of all the primers used to prepare these constructs are shown in Supplementary Table S1. The *bctrp1* gene knockout vector was constructed using the double-joint PCR method (Yu et al., 2004). The genomic DNA of *B. cinerea* TB-31 was extracted by the E.Z.N.A. Fungal DNA Mini kit (Omega, D3390-01, United States). With the DNA of TB-31 as the template, we amplified the 5' fragment (552 bp) and 3' fragment (613 bp) of the open reading frame (ORF) of *bctrp1* by the primer pairs *bctrp1*-5'F/-R and *bctrp1*-3'F/-R, respectively. The *hph* fragment was amplified using primer pairs *hph*-F/-R. With the primer pair *bctrp1*-5'F/3'-R to amplify the gene knockout cassette by overlapping PCR (Supplementary Figure S2A). The gene knockout cassettes were transformed into fungal protoplasts as described by Choquer et al. (2008). Transformants were selected on PDA containing hygromycin (50  $\mu$ g·mL<sup>-1</sup>), and three generations were purified on PDA with hygromycin. Transformants were verified

by PCR using the primers *bctrp1*-out-5'F/*hph*-in-R, *hph*-in-F/*bctrp1*-out-R, *hph*-F/-R, *bctrp1*-dectet-F/-R which were shown in Supplementary Table S1, and driven by real-time quantitative reverse transcription PCR (qRT-PCR) using the primers qRT-*bctrp1*-F/-R.

To further confirm that the differences in production of ABA between  $\Delta$ *Bcfrp1* and TB-31 were caused by the loss of *bctrp1*, we constructed the complementary vector pCBg1-*bctrp1* and then transformed it into a  $\Delta$ *Bcfrp1* mutant (Supplementary Figure S2A). We amplified *bctrp1* cDNA from *B. cinerea* TB-31 using the primers *bctrp1*-cde-F/-R, and cloned into the *ScaI* and *XbaI* digested sites in pCBg1 to generate pCBg1-*bctrp1*. The vector, pCBg1-*bctrp1*, was utilized for ATMT of the conidia of  $\Delta$ *Bcfrp1*. Transformants were selected on PDA that contained hygromycin (50  $\mu$ g·mL<sup>-1</sup>) and glyphosate (100  $\mu$ g·mL<sup>-1</sup>), and three generations were purified on PDA with hygromycin and glyphosate. The transformants were verified by PCR using the primers *bctrp1*-dectet-F/-R, *hph*-F/-R, Bar-in-F/-R, and qRT-PCR using the primers qRT-*bctrp1*-F/-R.

### 2.3. Phenotypic analysis of the deletion and complementation mutants of *bctrp1*

To detect the extracellular ABA in TB-31 and the  $\Delta$ *Bcfrp1* and  $\Delta$ *Bcfrp1*-C mutants, these strains were inoculated on PDA media for 6–12 days at 26°C. The detection of ABA yield was performed by high-performance liquid chromatography (HPLC) as described by Ding et al. (2015). The biomass was quantified by collecting the mycelia of the three strains from 50 ml of PDB after 72, 96 and 120 h. The mycelia were filtered and weighed after drying at 100°C for 60 min (Ding et al., 2016). The colony diameters of the TB-31 and mutant strains were analyzed on agar plates. Briefly, each strain was separately inoculated on Czapek–Dox agar (CDA) media with different sugar carbon sources: 2% D-glucose, 2% sucrose, 2% lactose, or 2% maltose, respectively, for 6 days at 26°C. Each strain was analyzed in triplicate.

### 2.4. Transcriptome sequencing and analysis

After culturing on PDA in the dark for 6 days at 26°C, the mycelia of the *B. cinerea* TB-31 and  $\Delta$ *Bcfrp1* were harvested and stored at -80°C. The total RNA was extracted using TRIzol according to the manufacturer's instructions (Invitrogen, Carlsbad, CA, United States). After the quality and concentration of RNA were tested and qualified, the RNA library was sequenced by Gene Denovo Biotechnology Co., Ltd. (Guangzhou, China) with the Illumina NovaSeq 6,000 (San Diego, CA, United States; Modi et al., 2021). The raw data that were obtained were filtered and mapped to the genome of model microorganism *B. cinerea* B05.10 (NCBI, ASM14353v4) using HISAT2.2.4 (Kim et al., 2015). The genes obtained were quantified using RNA-seq by expectation maximization (RSEM; Li and Dewey, 2011), and their levels of

expression were normalized using Fragments Per Kilobase of transcript per Million mapped reads (FPKM) as described by Li and Dewey (2011). The differential expression analysis was analyzed between TB-31 and  $\Delta$ Bcfrp1 by DESeq2 (Love et al., 2014). The differentially expressed genes (DEGs) were filtered based on fold change  $\geq 2$  and false discovery rate (FDR)  $\leq 0.05$  (FPKM  $> 1$ ). The gene functions were annotated against the cluster of orthologs/eukaryotic clusters of orthologs (COG/KOG), Gene Ontology (GO) and Kyoto Encyclopedia of Genes and Genomes (KEGG) database as described by Fang et al. (2021).

## 2.5. Proteome analysis

Consistent with the samples analyzed by transcriptome sequencing, the samples for proteome analysis were also harvested after 6 days of culture on PDA. The total protein of TB-31 and  $\Delta$ Bcfrp1 was extracted and measured with BCA (Bicinchoninic acid) method as described by Jia et al. (2022). The proteins were digested into peptide fractions and performed with the method of data-independent acquisition (DIA) as described by Jia et al. (2022). DIA raw data were performed by Spectronaut X (Biognosys AG, Schlieren, Switzerland) as described by Long (Long et al., 2020). All the selected precursors passing the filters were employed to quantify. The differentially expressed proteins (DEPs) were filtered based on fold change  $\geq 1.5$  and  $p < 0.05$  after subjecting them to Student's *t*-test. The protein function were annotated against COG/KOG, GO and KEGG database with  $p \leq 0.05$  as described by Wei et al. (2022).

## 2.6. Correlation analysis of genes and proteins

We have uploaded the Transcriptome and Proteome data in the ScienceDB (<https://www.scidb.cn/detail?dataSetId=bf230977945c4b4785ec355293b23d79>). First, the differentially expressed genes and proteins were identified between TB-31 and  $\Delta$ Bcfrp1. A significant DEG was screened with fold change  $\geq 2$  and FDR  $< 0.05$ , and a significant DEP was screened with fold change  $> 1.5$  and  $p < 0.05$ , respectively. Second, the correlation analysis between genes and proteins were analyzed as described by Dou et al. (2022). The Venn diagram was used to count the genes/proteins and the differential genes/differential proteins, respectively. The correlation analysis between genes and proteins were carried out by R language (version 3.5.1). In addition, the nine-quadrant map shows the functional enrichment with the GO and KEGG pathway analysis of mRNAs and proteins.

## 2.7. qRT-PCR analysis

All the mycelial RNA was extracted using TRIzol according to the manufacturer's instructions (Invitrogen, Carlsbad, CA,

United States). The quality and concentration of RNA was detected as described by Wang et al. (2018). cDNA was synthesized by the TaKaRa reverse transcriptase kit (TaKaRa, Dalian, China). The qRT-PCR was conducted using the AceQ qPCR SYBR Green master mix kit (Nanjing Vazyme Biotech Co., Ltd., Nanjing, China). The qRT-PCR primers in this study are shown in Supplementary Table S1. The reactions were conducted in a CFX96 real-time PCR detection system (Bio-Rad, Hercules, CA, United States). Each transcript was analyzed using three PCR repetitions in parallel. The tubulin gene (Bcin02g00900) served as an internal control (Dulermo et al., 2010). The fold change in the mRNA was analyzed by  $2^{-\Delta\Delta Ct}$  method.

## 3. Results

### 3.1. Identification ABA-deficient mutant named E154

*Botrytis cinerea* TB-31 was transformed with pBHT2, which is a commonly used binary vector for ATMT in filamentous fungi, to create ABA-deficient mutants by insertional mutagenesis. This plasmid enables the selection of hygromycin-resistant (*hph*) transformants. The ATMT resulted in 217 hygromycin-resistant transformants that were grown for 8 days on PDA media and tested for their production of ABA using HPLC. Among the positive transformants, one mutant designated E154 exhibited a reduction of approximately 40% in the yield of ABA compared with the parental strain TB-31 when cultured on PDA agar for 6 days (Supplementary Figure S1A). However, the E154 mutant had a similar colony morphology when compared with TB-31 (Supplementary Figure S1B).

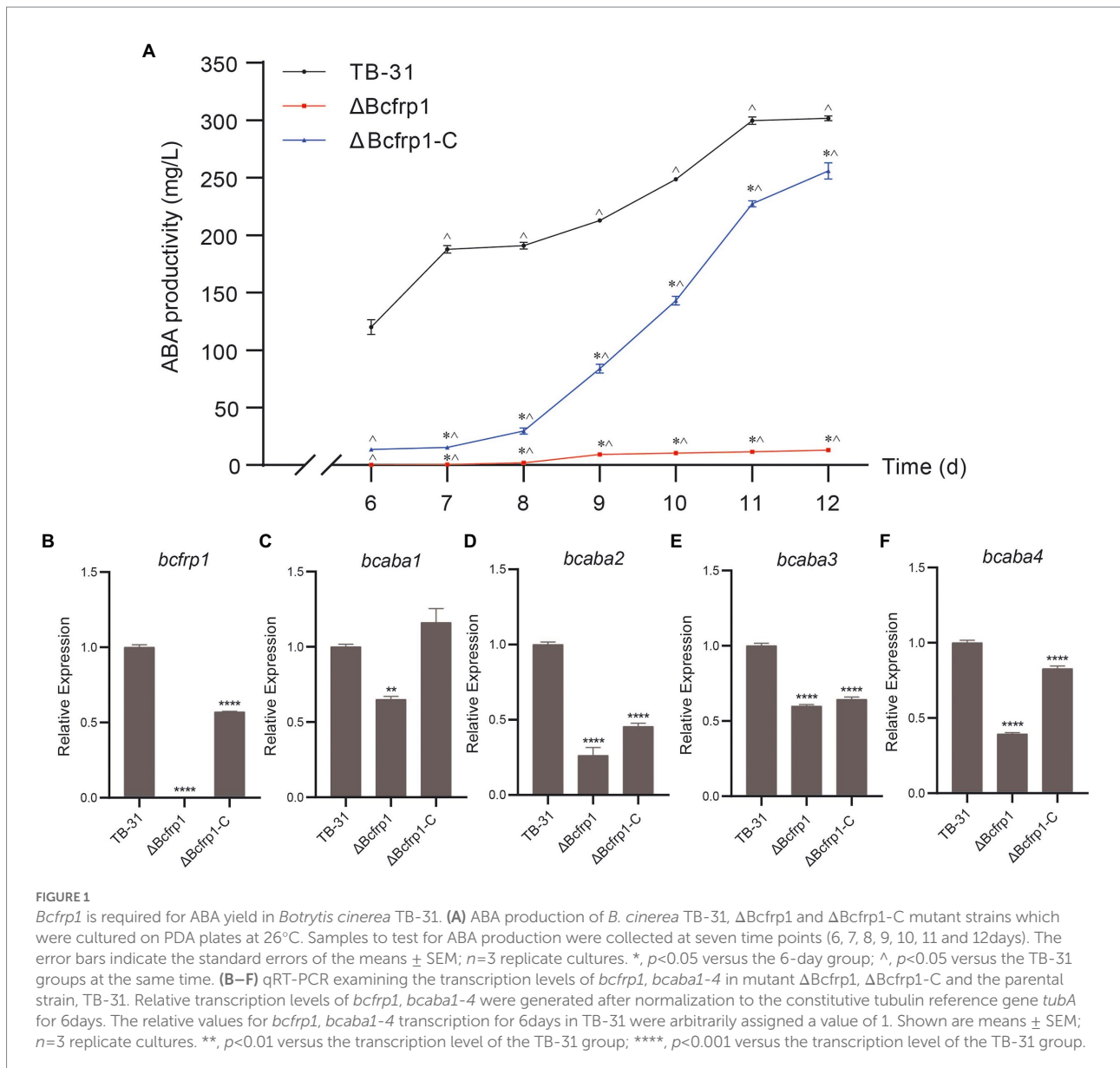
Thermal asymmetric interlaced PCR (TAIL-PCR) was carried out to isolate the portion of the genome that is close to either the right or left boundary of the T-DNA integration event as described from rice blast (*Magnaporthe oryzae*; Chen et al., 2011). In this study, we found that T-DNA was integrated in TB-31 at 1806bp upstream of the predicted start codon of BC\_5\_05922 (Supplementary Figure S1C; Supplementary Table S2). A reverse transcription (RT)-PCR assay showed that the level of transcription of BC\_5\_05922 decreased significantly in the E154 mutant (Supplementary Figure S1D). The full-length DNA and cDNA were also isolated for BC\_5\_05922 from TB-31, and the complementary assay showed that the reduction of ABA could be complemented in *trans* by integrating a functional copy of the BC\_5\_05922 cDNA into the E154 strain using the vector pCBg1 (Supplementary Figure S1A). In addition, it showed that the translated protein of BC\_5\_05922 had 100% amino acid identity with Bcfrp1 (BCIN\_11g00230) of *B. cinerea* B05.10 using the BLASTP algorithm from NCBI. These findings suggested that T-DNA integration upstream of the *befr1* gene may be linked to the E154 phenotype.

### 3.2. *bctrp1* is required for the biosynthesis of ABA in *Botrytis cinerea* TB-31

To confirm that *bctrp1* is required for the biosynthesis of ABA by *B. cinerea* TB-31, we knocked out the *bctrp1* gene and replaced the endogenous *bctrp1* ORF with the *hph* gene. Moreover, we performed qRT-PCR and diagnostic PCR assays to confirm the *bctrp1* gene was disrupted in the  $\Delta$ Bctrp1 mutant (Supplementary Figure S2B). The productivity of  $\Delta$ Bctrp1 for ABA decreased significantly by approximately 97% compared with TB-31 on PDA for 12 days (Figure 1A). To further confirm that the differences in the amount of ABA produced between TB-31 and  $\Delta$ Bctrp1 was due to the loss of *bctrp1*, we constructed the complementation vector pCBg1-*bctrp1* and then transformed it into the mutant  $\Delta$ Bctrp1 to generate the complementary mutant

$\Delta$ Bctrp1-C (Supplementary Figure S2C). The amount of ABA produced by  $\Delta$ Bctrp1-C returned to 85% of that of the control, TB-31, when cultured on a PDA plate for 12 days (Figure 1A).

Furthermore, the qRT-PCR trial verified that *bctrp1* was disabled by deleting in the mutant  $\Delta$ Bctrp1. The levels of transcription of *bctrp1* in  $\Delta$ Bctrp1-C were restored to approximately 57% of that produced by TB-31 when grown on a PDA plate for 6 days (Figure 1B). To investigate whether *bctrp1* was involved in the regulation of ABA gene clusters, we conducted qRT-PCR to analyze the levels of transcription of *bcaba1-4* among the *B. cinerea* strains (Figures 1C–F). The levels of transcription of the *bcaba1-4* in  $\Delta$ Bctrp1 were decreased to 75, 26, 60 and 40% of TB-31, respectively (Figures 1C–F). Each level of gene expression increased when ABA performance was re-established in  $\Delta$ Bctrp1-C, which suggests that the deletion of *bctrp1* affects the



transcription of *bcaba1-4*. Combining with the previous data of insertional mutagenesis confirmed that *bcfrp1* is required for the biosynthesis of ABA in TB-31.

### 3.3. Bcfrp1 disrupts the normal growth of *Botrytis cinerea* TB-31

We compared the morphology and radial growth of *B. cinerea* TB-31,  $\Delta$ Bcfrp1, and  $\Delta$ Bcfrp1-C cultured on PDA. The growth rate of hyphae in  $\Delta$ Bcfrp1 mutant slowed down and no matter how long it takes to cultivate, the hyphae of  $\Delta$ Bcfrp1 could not be extended to the whole plate like TB-31. The hyphae of  $\Delta$ Bcfrp1 also became lighter and had sporadic whiteness. The mycelial layer of  $\Delta$ Bcfrp1 became thinner, with the decrease in the number of conidia compared with those of TB-31. Simultaneously, the introduction of the *bcfrp1* cDNA into  $\Delta$ Bcfrp1 restored the wild-type morphology and growth phenotypes, confirming that this mutant had been complemented (Figures 2A,B). The results showed that *bcfrp1* was positive for the hyphal growth of TB-31. Moreover, we compared the biomass of three strains grown on PDB media. The biomass of  $\Delta$ Bcfrp1 mutant decreased to 56.5% of TB-31 after 120h of culture on PDB, while the biomass of  $\Delta$ Bcfrp1-C mutant was close to that of the parental strain TB-31 on PDB media (Figure 2C). These results suggested that *bcfrp1* was important for maintaining the normal growth of TB-31.

In addition, we compared the colony diameters of TB-31,  $\Delta$ Bcfrp1, and  $\Delta$ Bcfrp1-C on CDA media for 6 days with several carbon sources (Figure 2D). As shown in Figure 2E, the colony diameter of the  $\Delta$ Bcfrp1 mutant cultured on CDA with 2% D-glucose, 2% maltose, and 2% lactose as carbon sources was 1.5, 1.5 and 3.5 cm, respectively. Moreover,  $\Delta$ Bcfrp1 could not grow on CDA plates that contained sucrose. Moreover, the colony size of  $\Delta$ Bcfrp1 in different carbon sources could be recovered to varying degrees through complementation with *bcfrp1*.

### 3.4. The transcriptomics and proteomics analysis of *Botrytis cinerea* TB-31 and $\Delta$ Bcfrp1

To further analyze the dynamic changes in the levels of expression of genes and proteins after the deletion of the *bcfrp1* gene in *B. cinerea* TB-31, mycelial samples of TB-31 and  $\Delta$ Bcfrp1 were collected after cultivation on PDA media for 6 days and subjected to transcriptome and proteome analyses, respectively.

High-throughput RNA sequencing (RNA-seq) generated more than 30 million clean reads for each sample, and three biological replicates were performed for each group. As a result, 12,303 genes were detected in the library, and there are 11,707 genes in the whole genome. The other 596 genes are newly predicted genes. In total, 4,128 (2,661 upregulated and 1,647 downregulated) were identified as DEGs ( $\log_2$ ratio > 1) in TB-31

(as the control) vs.  $\Delta$ Bcfrp1 (Figure 3A). 15 genes were randomly selected for qRT-PCR analysis to verify RNA-seq data (Figure 3B), and the gene expression levels measured by the two methods were linearly correlated ( $r_{\text{pearson}} = 0.8376$ ).

To examine the proteins altered by *bcfrp1*, proteomic profiles were analyzed between TB-31 and  $\Delta$ Bcfrp1 with three biological replicates. In total, 45,527 peptides and 5,645 proteins were identified in the proteomes of TB-31 and  $\Delta$ Bcfrp1. A Pearson correlation analysis was highly repeatable and reliable (Pearson > 0.97) among the three biological replicates (Figure 3C). A total of 1,073 DEPs ( $\log_2$ ratio > 0.58) were observed. A total of 446 proteins were downregulated, and 627 proteins were upregulated in the mutant group compared with the TB-31 group ( $p < 0.05$ ; Figure 3A).

### 3.5. Correlation analysis of transcriptome and proteome

The transcriptome and proteome data were performed with a global correlation analysis. In Figure 4A, a total of 5,615 proteins matched the transcripts, including 1,067 which were DEPs, 2,101 which were DEGs, and 552 were shared as both DEPs and DEGs. In Figure 4B, the nine-quadrant diagram shows that there are 941 NDEGs/NDEPs in quadrant 5. The 268 and 98 candidate proteins were DEGs which differentially transcribed in quadrant 1 and quadrant 9, respectively. The 81 and 86 candidate proteins were DEPs which were not differentially transcribed in quadrant 4 and quadrant 6, respectively. The 12 and 10 candidate proteins had the opposite patterns of expression from their transcripts in quadrant 1 and quadrant 9, respectively. In addition, the 103 and 32 candidate proteins showed the same expression patterns as the transcripts in the quadrants 3 and 7, respectively.

We performed pathway enrichment using the KEGG to explore the possible pathways which may be affected by *bcfrp1*. The results showed that the most DEGs/DEPs were enriched in Metabolic pathways (368 DEGs/ 215 DEPs), and the Biosynthesis of secondary metabolites (153 DEGs/ 97DEPs), and Biosynthesis of amino acids (36 DEGs/ 23 DEPs; Figure 4C). As shown in Figures 4D,E, the DEG/DEP pairs in quadrant 3 and 7 were mainly enriched in the pathways of Metabolic, Secondary metabolites, and Starch and sucrose metabolism.

To screen out the pathways that may play important roles with *bcfrp1*, we performed a pathway enrichment analysis based on the KEGG database. The results showed that the most DEGs/DEPs were involved in metabolic pathways (ko01100, 368 DEGs/ 215 DEPs), followed by the biosynthesis of secondary metabolites (ko01110, 153 DEGs/ 97DEPs), and biosynthesis of amino acids (ko01230, 36 DEGs/ 23 DEPs; Figure 4C). As shown in Figures 4D,E, the DEG/DEP pairs in quadrant 3 and 7 were mainly enriched in the metabolic pathways (ko01100), biosynthesis of secondary metabolites (ko01110), starch and sucrose metabolism (ko00500).

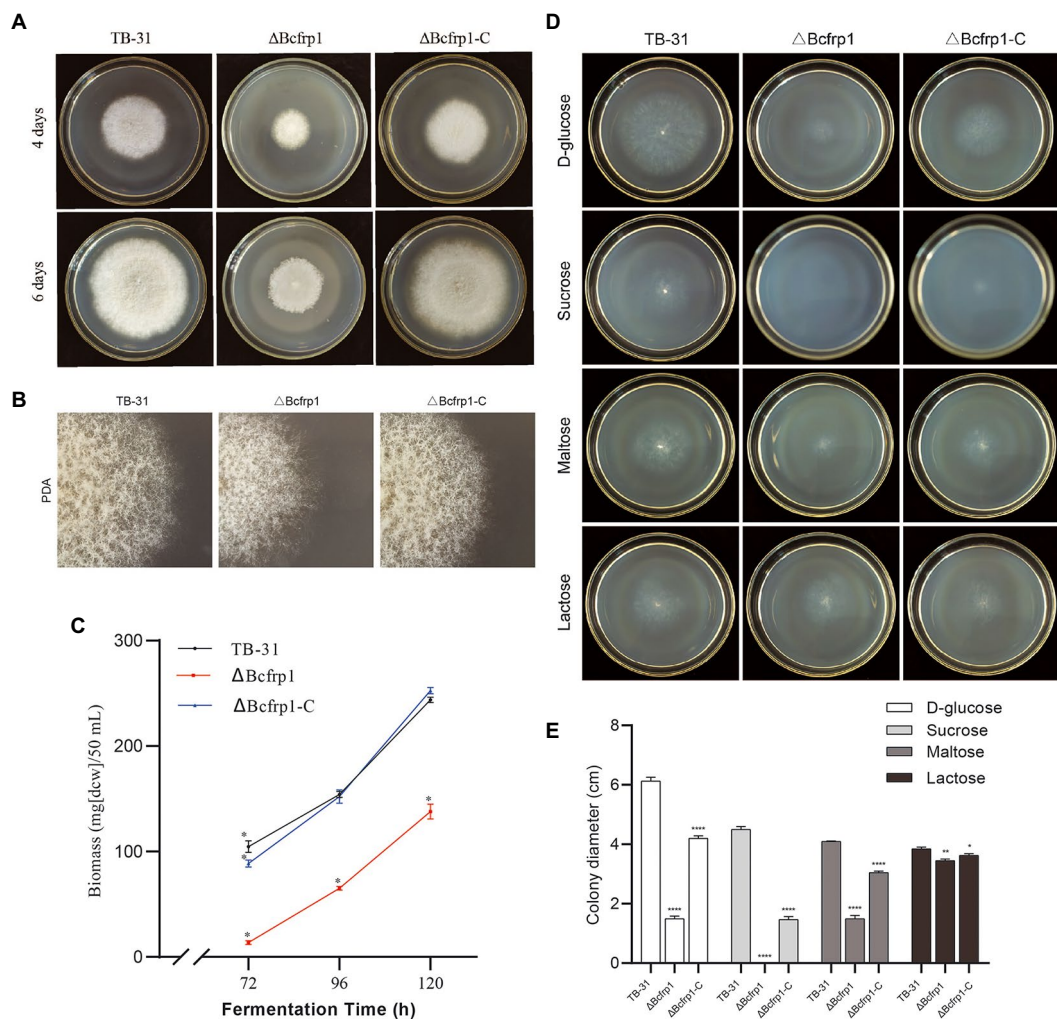


FIGURE 2

The biomass and colony morphology of *B. cinerea* TB-31,  $\Delta$ Bcfrp1 and  $\Delta$ Bcfrp1-C. (A) The morphology of TB-31,  $\Delta$ Bcfrp1 and  $\Delta$ Bcfrp1-C on PDA media for 4 days and 6 days. (B) The morphology of TB-31,  $\Delta$ Bcfrp1 and  $\Delta$ Bcfrp1-C on PDA media for 4 days and 6 days. All images were captured at 3X magnification. (C) Biomass of TB-31,  $\Delta$ Bcfrp1 and  $\Delta$ Bcfrp1-C on PDB media at 26°C at 180rpm on an orbital shaker. The mycelia were collected at three time points (72, 96, and 120h). Shown are means  $\pm$  SEM;  $n=3$  replicate cultures. \*,  $p<0.05$  versus the biomass of the TB-31 group. (D) The colony morphology of TB-31,  $\Delta$ Bcfrp1 and  $\Delta$ Bcfrp1-C on CDA media with 2% D-glucose, 2% Sucrose, 2% Maltose, and 2% Lactose plates and cultured at 26°C for 6 days. (E) Colony diameters of the TB-31,  $\Delta$ Bcfrp1 and  $\Delta$ Bcfrp1-C strains on CDA media with 2% D-glucose, 2% Sucrose, 2% Maltose, and 2% Lactose cultured at 26°C for 6 days. Shown is means  $\pm$  SEM;  $n=3$  replicate cultures. \*,  $p<0.05$  versus colony sizes of the TB-31 group; \*\*,  $p<0.01$  versus the transcription level of the TB-31 group; \*\*\*\*,  $p<0.001$  versus the transcription level of the TB-31 group.

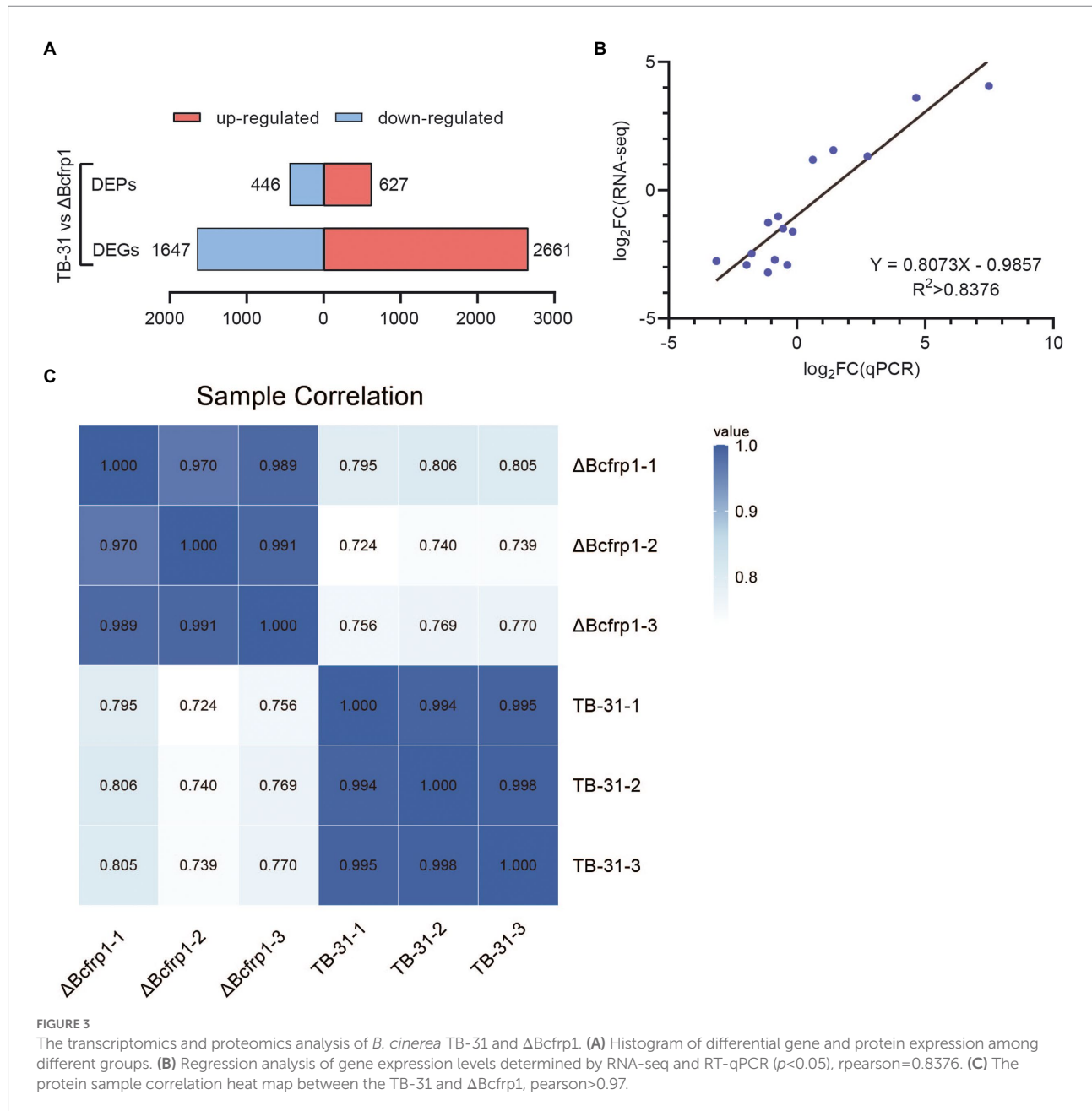
### 3.6. DEGs and DEPs involved in putative sugar transport and degradation

We found the DEGs and DEPs involved in putative sugar transport and degradation were significantly changed for expression between *B. cinerea* TB-31 and  $\Delta$ Bcfrp1 (Figure 5; Supplementary Table S3).

Monosaccharide (glucose) and disaccharide (maltose, sucrose and lactose), as nutrients of fungi, can be transported to fungal cells through sugar transporters. Several genes that encode sugar transporters, including three major facilitator superfamily (MFS) sugar transporters (Bchex3, Bchex5, and Bchex6), a glucose transporter *rco-3*, a glucose/galactose transporter *gluP*, and a

fructose proton symporter (*BcFrt1*) were upregulated at both the transcription and translation levels in  $\Delta$ Bcfrp1 compared with TB-31 ( $p<0.05$ ), while a gene that encoded an MFS sugar transporter (*Bchex1*) was upregulated at the translation level. In addition, a gene that encoded a protein similar to a sucrose transporter *Sut1* was downregulated at both the transcription and translation levels, and two genes that encoded the maltose transporters *MAL11* and *MAL61* were downregulated at the transcription levels.

The transcriptome and proteome analysis also revealed that the genes that encoded two  $\alpha$ -amylase enzymes (*Bcin02g01420* and *Bcin04g06250*), two  $\alpha$ -glucosidase enzymes (*Bcin14g00650* and *Bcin12g03390*), glycoamylase (*Bcgs1*), and four glycoside



hydrolases (Bcin08g02110, Bcin16g03950, Bcin03g08710, and Bcin14g00480) were upregulated at both the transcription and translation levels in  $\Delta Bcfrp1$  compared with those of TB-31 ( $p < 0.05$ ). Moreover, the genes that encoded a glycosyl hydrolase (Bcin10g05710), an  $\alpha$ -galactosidase (Bcin03g02710) and a  $\beta$ -galactosidase (Bcin06g04500) were upregulated at the translation levels, while a galactose oxidase (Bcin09g04410) was upregulated at both the transcription and translation levels. These enzymes could be involved in the degradation of starch, sucrose, cellulose, and lactose, respectively. However, the level of translation of the genes that encoded the enzymes for glycogen degradation, such as a glycogen debranching enzyme (Bcgdb1), a glycogen phosphorylase (Bcgph1), and an ADP-sugar

bisphosphatase (Bcin08g01920) were downregulated in  $\Delta Bcfrp1$  compared with TB-31 ( $p < 0.05$ ).

### 3.7. DEGs and DEPs involved in ABA biosynthesis-related pathways

We analyzed the DEGs and DEPs involved in ABA biosynthesis-related pathways in *B. cinerea* TB-31 and  $\Delta Bcfrp1$  (Figure 6; Supplementary Table S4).

The carbon flux from glucose to pyruvate via catabolic glycolysis and pentose phosphate pathway (PPP), and the genes that encoded hexokinase (Bcglk), transaldolase (Bcin09g03850)

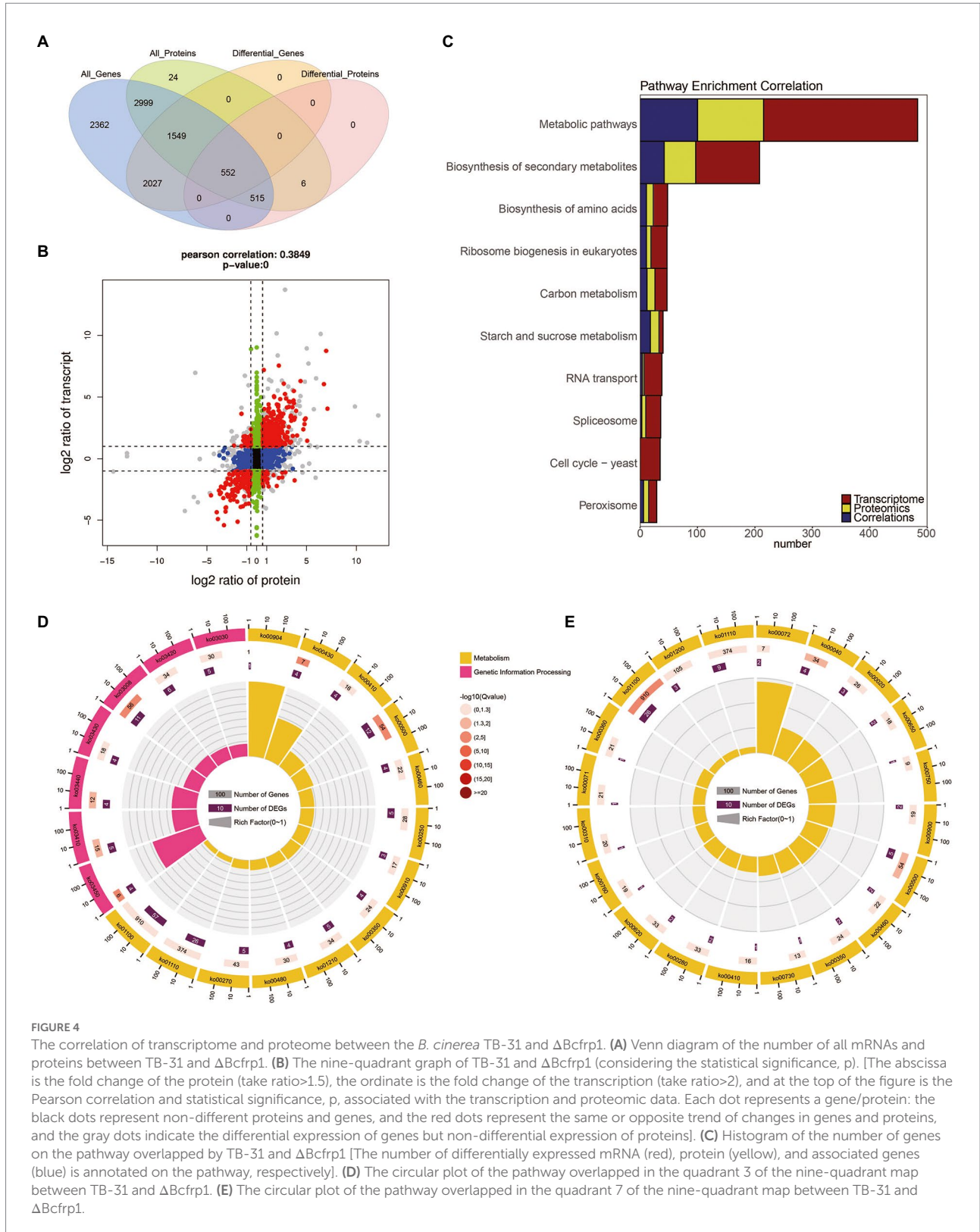


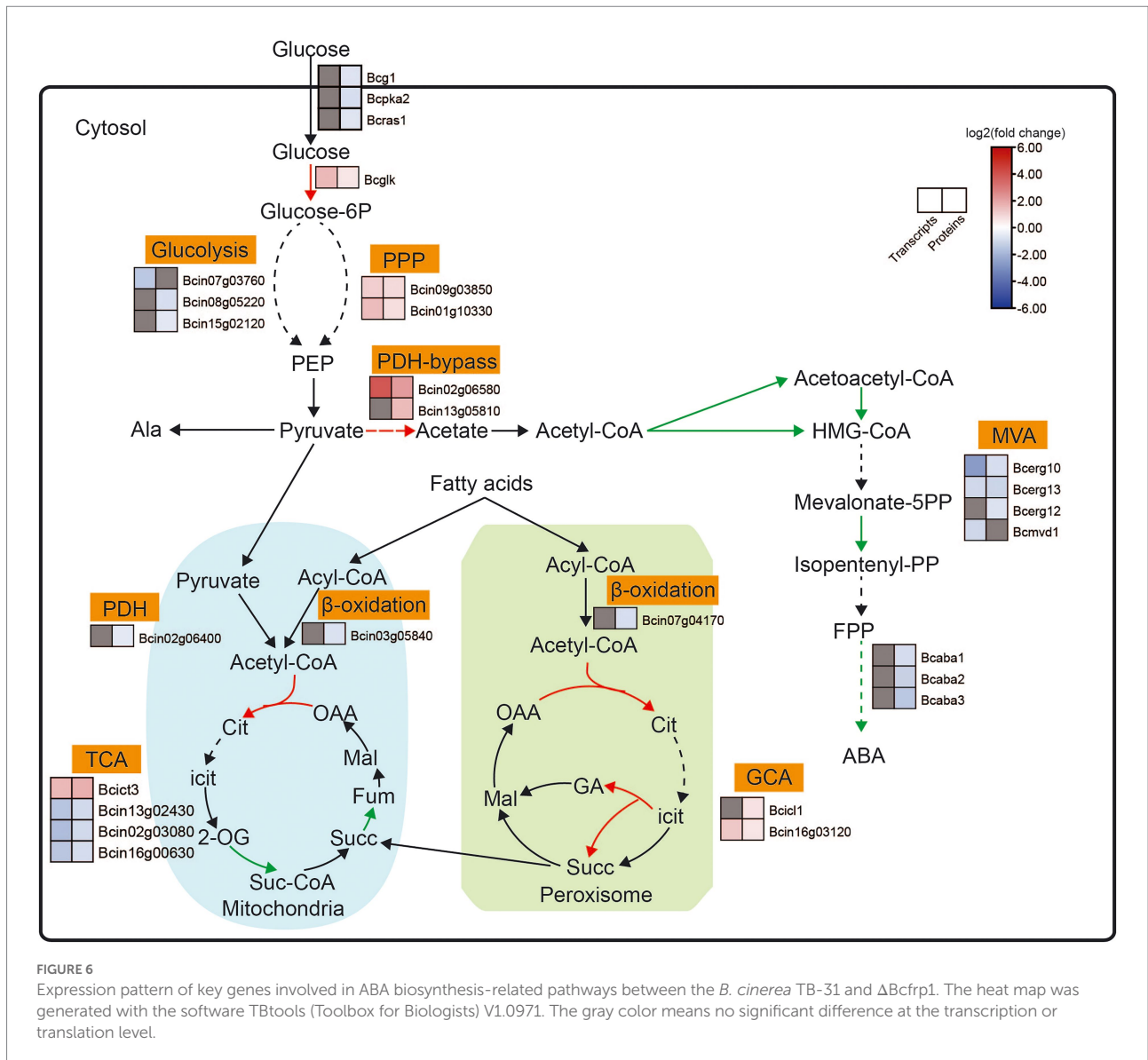
**FIGURE 4**

The correlation of transcriptome and proteome between the *B. cinerea* TB-31 and  $\Delta$ Bcfrp1. **(A)** Venn diagram of the number of all mRNAs and proteins between TB-31 and  $\Delta$ Bcfrp1. **(B)** The nine-quadrant graph of TB-31 and  $\Delta$ Bcfrp1 (considering the statistical significance, p). [The abscissa is the fold change of the protein (take ratio>1.5), the ordinate is the fold change of the transcription (take ratio>2), and at the top of the figure is the Pearson correlation and statistical significance, p, associated with the transcription and proteomic data. Each dot represents a gene/protein: the black dots represent non-different proteins and genes, and the red dots represent the same or opposite trend of changes in genes and proteins, and the gray dots indicate the differential expression of genes but non-differential expression of proteins]. **(C)** Histogram of the number of genes on the pathway overlapped by TB-31 and  $\Delta$ Bcfrp1 [The number of differentially expressed mRNA (red), protein (yellow), and associated genes (blue) is annotated on the pathway, respectively]. **(D)** The circular plot of the pathway overlapped in the quadrant 3 of the nine-quadrant map between TB-31 and  $\Delta$ Bcfrp1. **(E)** The circular plot of the pathway overlapped in the quadrant 7 of the nine-quadrant map between TB-31 and  $\Delta$ Bcfrp1.

and DAHP synthetase I (Bcin01g10330) were upregulated at both the transcription and translation levels in  $\Delta$ Bcfrp1 compared with TB-31 ( $p < 0.05$ ). However, the levels of translation of two genes that encoded triosephosphate isomerase (Bcin08g05220) and

glyceraldehyde-3-phosphate dehydrogenase (Bcin15g02120) were downregulated, respectively. Moreover, one gene that encoded fructose-bisphosphate aldolase (Bcin07g03760); was downregulated at the transcription level in  $\Delta$ Bcfrp1 compared





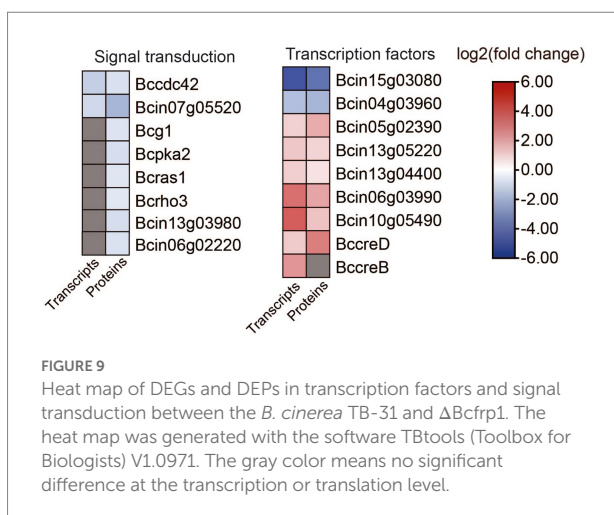
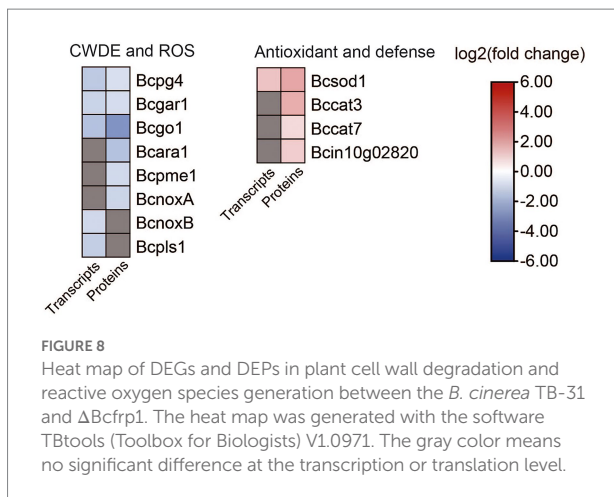
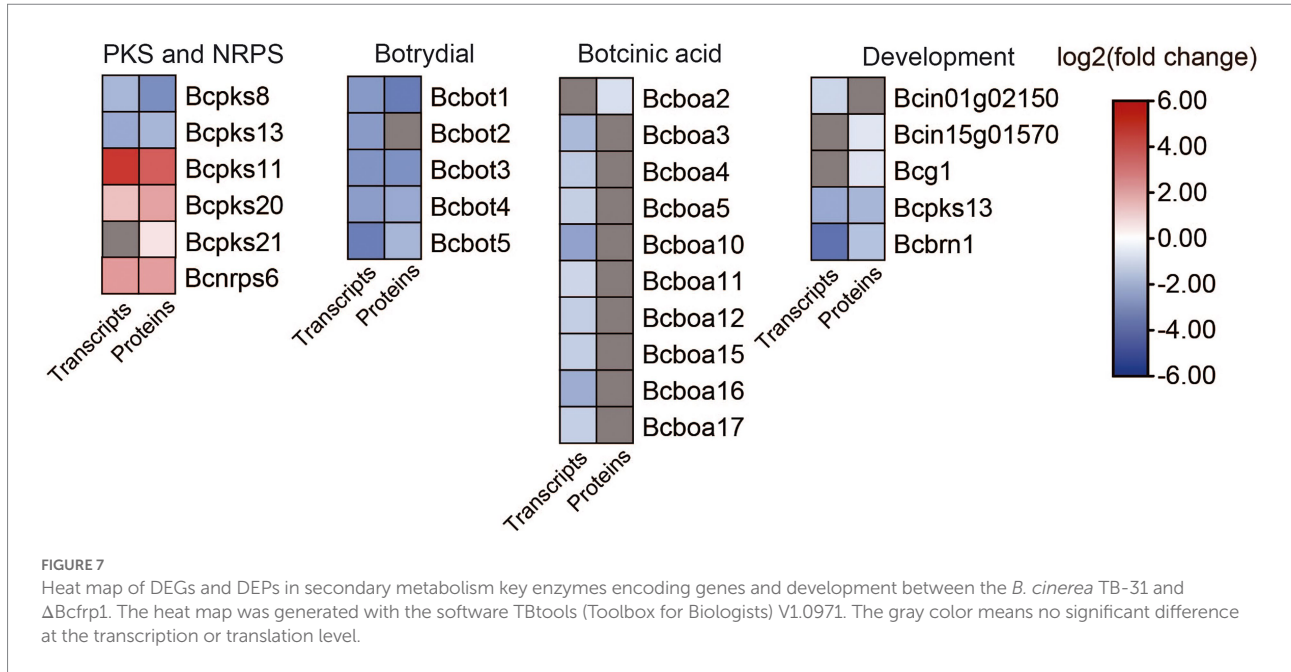
that three polyketide synthase genes including Bcpgs13, hydroxynaphthalene reductase dehydrates (Bcbrn1) and scytalone dehydratase (Bcscd1) were involved in the synthesis of DHN melanin (Zhang et al., 2015). In this study, the *bcpks13* and *bcbrn1* genes were downregulated at both the transcription and translation levels in  $\Delta$ Bcfrp1 compared with those in TB-31 ( $p < 0.05$ ), while the *bcsd1* gene was upregulated at both the transcription and translation levels.

### 3.10. DEGs and DEPs involved in plant cell wall degradation and the generation of reactive oxygen species

It was reported that the gene *fofrp1* is required for pathogenicity in *Fusarium oxysporum* (Jonkers et al., 2011). We analyzed the transcriptome and proteome data between

*B. cinerea* TB-31 and  $\Delta$ Bcfrp1, and the results showed that; except for the genes involved in the synthesis of BOA and BOT toxins, there were also a considerable number of genes involved in pathogenicity that were differentially expressed (Figure 8; Supplementary Table S7).

While invading their hosts, many phytopathogenic fungi synthesize plant cell wall degrading enzymes (CWDE), for example xylanases, pectinases, and arabinanase (Amselem et al., 2011). Extracellular enzymes have been selected as potential virulence factors due to promoting the growth of hyphae. Three genes that encoded an endopolygalacturonase (Bcpg4), a galacturonate reductase (Bcgar1), and a glyoxal oxidase (Bcgo1) were downregulated at both the transcription and translation levels in  $\Delta$ Bcfrp1 compared with those in TB-31 ( $p < 0.05$ ). Moreover, the two genes that encoded  $\alpha$ -1,5-L-endo-arabinanase (Bcara1) and pectin methylesterase (Bcpme1), were downregulated at the translation level.



*Botrytis cinerea* is a necrotrophic pathogen that can generate reactive oxygen species (ROS) by enzymes. NADPH oxidases (Nox) are major enzyme systems that produce ROS, which can contribute to the virulence of the fungus. Siegmund et al. (2013) reported that the Nox including a tetraspanin (BcPls1) and two catalytic transmembrane subunits (BcNoxA, BcNoxB) were required for the virulence involved in the process of penetration in *B. cinerea* (Siegmund et al., 2013). In this study, the translation levels of *bcnoxA* were downregulated, while transcription levels of *bcnoxB* and *bcpls1* were downregulated in  $\Delta$ Bcfrp1 compared with TB-31 ( $p < 0.05$ ), which could affect the penetration of  $\Delta$ Bcfrp1. In addition, the antioxidant enzymes can protect fungi by degrading the ROS produced by plants. In this study, the superoxide dismutase gene (*Bcsod1*) was upregulated at both the transcription and translation levels, and the catalase (*Bccat3* and *Bccat7*) and glutathione S-transferase kappa 1 (*Bcin10g02820*) genes were upregulated at the translation level in  $\Delta$ Bcfrp1 compared with that of TB-31 ( $p < 0.05$ ). Thus, we speculated that the upregulation of antioxidant enzymes could protect the fungal cell from the ROS.

### 3.11. Analysis of transcription factors and other genes associated with signal transduction

Eight genes that are involved in signal transduction were differentially expressed in  $\Delta$ Bcfrp1 compared with TB-31 ( $p < 0.05$ ; Figure 9; Supplementary Table S8). Two genes that encode the cell division control protein 42 (*Bccdc42*) and calmodulin (*Bc4*) were downregulated at both the transcriptional and translational levels. In addition, six genes were downregulated at the translational level, including the genes that encode

heterotrimeric G  $\alpha$ -subunit (Bcg1), PKA catalytic subunit (Bcpka2), medium Ras-like GTPase (Bcras1), small GTPase (Bcrho3), MAPK p21-activated kinase (Bcste20), and serine/threonine protein phosphatase pzh1.

In addition, nine genes that encode transcription factors (TFs) were differentially expressed in  $\Delta$ Bcfrp1 compared with TB-31 ( $p < 0.05$ ; Figure 9; Supplementary Table S8). Of them, two genes that encode cutinase A (BccutA) and the regulatory subunit of protein phosphatase 1 Bcglc8, respectively, were downregulated at both the transcriptional and translational levels. Six genes that encoded TFs (Bcsfp1, Bctma46, Bcin13g04400, Bcku70, Bcku80, and BccreD) were upregulated at both the transcriptional and translational levels. In addition, a gene that encoded BccreB, a TF that is involved in the process of deubiquitinating CreA, was upregulated at the transcriptional level.

## 4. Discussion

The ubiquitin-proteasome system (UPS) is the main pathway for the degradation of intracellular protein in eukaryotes, which is composed of ubiquitin, ubiquitin-activating enzyme E1, ubiquitin-conjugating enzyme E2s, ubiquitin ligase E3s, 26S proteasome, and deubiquitinates (DUBs; Willems et al., 2004; Wu et al., 2022). SCFs complexes constitute a new class of E3 ligases, in which F-box protein is responsible for regulating its downstream target proteins by specific recognition and ubiquitination of protein substrates (Cardozo and Pagano, 2004; Johnk et al., 2016). The fungal F-box protein was initially found in *Saccharomyces cerevisiae*, and has been shown to play an important role in regulating a variety of cellular functions, including cell cycle regulation, nutritional sensing and fungal morphogenesis in fungi (Jonkers and Rep, 2009a; Sharma et al., 2021; Wu et al., 2022). For example, MUS-10 of *Neurospora crassa* is involved in cell senescence (Kato et al., 2010), Fbx23 and Fbx47 of *Aspergillus nidulans* participate in carbon catabolite repression (CCR), and Fbx50 (GrrA) is required for production of mature ascospores (De Assis et al., 2018). The F-box proteins are also required for virulence, like Fbx15 of *Aspergillus fumigata* and Fbp1 of *Cryptococcus neoformans* (Liu et al., 2011; Johnk et al., 2016). Frp1 is an F-box protein, which was initially found in *Fusarium oxysporum*, and its homologous proteins seem to show different functions in different fungi. Jonkers et al. (2011) reported that the F-box protein that encoded the gene *fofrp1* is necessary for virulence and carbon catabolism in *Fusarium oxysporum*, and the *B. cinerea* Bcfrp1 complemented into the  $\Delta$ Fofrp1 mutant restored pathogenicity (Jonkers et al., 2011). However, there is no effect on pathogenicity and sexual reproduction was impaired in the  $\Delta$ Bcfrp1 mutant produced by *B. cinerea* B05.10 (Jonkers et al., 2011). In our study, we found that a novel function of *bctfrp1* is required for the biosynthesis of ABA in *B. cinerea* TB-31. In this research, the mutant E154 that produced lower amounts of ABA revealed that the T-DNA insertion site was 1806bp upstream of the predicted start codon of Bcfrp1. In addition, the deletion of

Bcfrp1 had a significant effect on the biosynthesis of ABA in *B. cinerea* TB-31, and its yield decreased by 97% compared with TB-31 at 12 days. ABA yield of both E154-C and  $\Delta$ Bcfrp1-C restored to more than 80% by the complementation of *bctfrp1* gene. Although it did not reach the level of the control strain TB-31, which may be owing to the promoter sequence of *bctfrp1*, it was obvious that BcLAE1 was essential for ABA synthesis. To date, no reports have been published on the impact of F-box proteins on secondary metabolic regulation in *B. cinerea*.

To understand the evolution of Bcfrp1, we analyzed the conserved domain of F-box. The exact location of the F-box is 169–209 aa, defined as a receptor for ubiquitination targets (Supplementary Figure S3). A phylogenetic tree was constructed using the amino acids of the full length (Supplementary Figure S4), and resulted in the conclusion that orthologs of Bcfrp1 are present in fungi from six classes (Leotiomycetes, Sordariomycetes, Dothideomycetes, Eurotiomycetes, Pezizomycetes, and Xylonomycetes) belonging to the Pezizomycotina, and what's interesting is that these fungi are pathogenic fungi, such as *Sclerotinia sclerotiorum*, *Hyaloscypha bicolor*, *Venustampulla echinocandica*, *Neurospora crassa*, *Trichoderma reesei*, *Fusarium graminearum*, *Fusarium oxysporum* f. sp. *lycopersici*, *Trematosphaeria pertusa*, *Xylona heveae*, *Tuber melanosporum*. Bcfrp1 orthologs were relatively close to *Botrytis porri*, *Botrytis byssoidea*, *Botrytis sinoalii*, *Botrytis fragariae* and *Sclerotinia sclerotiorum*, which might share an ancestor. It is not clear whether these strains have the capability to produce ABA. These homologous proteins were not characterized in the present study but may be involved in functional gene regulation related to pathogenicity in these pathogenic fungi. The mechanism underlying the functions of Bcfrp1 and its homologues are still to be elucidated.

It is apparent that different *frp1* mutant have phenotypic variations which indicate that Frp1 targets different proteins in different fungi. However, Jonkers and Rep (2009a,b) speculated that the main function of Frp1 does not depend on ubiquitination of targets (Jonkers and Rep, 2009a). They found Frp1 of *F. oxysporum* can bind to Skp1 in yeast two-hybrid and pull-down assays, but mutations in the F-box domain of Frp1 that impair binding to Skp1 do not affect the phenotype. Therefore, in order to better understand the downstream genes affected by Frp1, a stringent comparative transcriptome and proteome analysis was performed to identify differentially expressed genes between TB-31 and  $\Delta$ Bcfrp1, which would be very useful for novel target genes discovery. We found about 627 upregulated DEPs and 446 downregulated DEPs between TB-31 and  $\Delta$ Bcfrp1, and 552 proteins were shared between both DEPs and DEGs, suggesting the changes in the transcriptomic and proteomic level is very notable. This study will help us find targets that may be regulated by *bctfrp1* and expand our knowledge of the molecular basis by which *bctfrp1* regulates ABA biosynthesis in *B. cinerea*.

We first compared data from the transcriptome and proteome to analyze the DEGs related to the ABA biosynthetic pathway. In  $\Delta$ Bcfrp1 mutant, several genes involved in the biosynthesis of

pyruvate and acetyl-CoA were upregulated at the transcription and/or translation level, which definitely favor the synthesis of acetyl-CoA. However, the levels of transcription and/or translation of the genes involved in IPP synthesis (MVA pathway), and the *bcaba1-4* genes involved in ABA synthesis from FPP were severely downregulated. As a result, we hypothesized that this is an important reason for the decrease of ABA biosynthesis in  $\Delta$ Bcfrp1 mutant. As Wang et al. (2018) reported the TF BcabaR1 directly regulate the promoter of ABA gene cluster (Wang et al., 2018). In this study, we found that the levels of transcription and translation of *bcabaR1* in  $\Delta$ Bcfrp1 did not change significantly when compared with TB-31. However, the levels of transcription of the entire ABA gene cluster were downregulated, so we speculated that there are other undiscovered regulatory mechanisms participating in the biosynthesis of ABA.

In addition to ABA, we also closely examined the other enzymes in secondary metabolism. The levels of transcription and translation of five key genes for enzymes were altered, including Bcpks8, Bcpks11, Bcpks13, Bcpks20, and Bcnrps6. The corresponding compounds of Bcpks8, Bcpks11 and Bcpks20 have not been identified. The level of translation of the sesquiterpene cyclase Bcbot2 gene was also downregulated, which is required for the virulence factor botrydial (BOT) biosynthesis. The biosynthetic gene cluster of BOT was similar to ABA, the remaining four genes in the BOT synthesis gene cluster (*bcbot1-5*) were downregulated at the levels of transcription and translation, while had no effect on TF Bcbot6. However, the deletion of Bcfrp1 resulted in the downregulation of Bcbot1-5 genes but not Bcbot6, implying that Bcfrp1-induced clustering regulation could have another mechanism to bypass the TF. In addition, the level of transcription of nine genes in the bocinic acid (BOA) gene cluster decreased. In a previous study, we found that the regulator BclaeA is essential for the biosynthesis of ABA, which could affect the levels of transcription of the ABA, BOT, and BOA clusters (Wei et al., 2022). In this study, the levels of transcription and translation of *bclaeA* in  $\Delta$ Bcfrp1 did not change noticeably compared with TB-31, indicating that there are different regulatory mechanisms for BclaeA to synthesize ABA.

The downregulation of the BOA and BOT gene clusters may affect the virulence of *B. cinerea*. Dalmais et al. (2011) knocked out two genes, Bcbot1 and Bcbot2, involved in BOT production in the wild-type strain T4, which resulted in reduced virulence. In addition, they simultaneously knocked out the key genes that encode the enzymes Bcboa6 or Bcboa9 of BOA in the strain B05.10 led to the reduction of virulence (Dalmais et al., 2011). In this study, the level of expression for Bcboa6 or Bcboa9 did not change in  $\Delta$ Bcfrp1 compared with TB-31. However, several genes that encoded plant CWDE and NADPH oxidase enzymes, were downregulated at the transcription and/or translation levels in  $\Delta$ Bcfrp1, suggesting that Bcfrp1 plays key roles in regulating the level of expression of these genes.

Simultaneously, we found that the radial growth was decreased in the Bcfrp1 mutants. The mycelia of the  $\Delta$ Bcfrp1 transformants appeared white when compared with that of TB-31 owing to

decreased expression of the key synthetic genes of melanin. The dihydroxynaphthalene (DHN) melanin biosynthetic pathway in *B. cinerea* comprises of the polyketide synthase PKS12 and PKS13, the hydrolase YGH1, tetrahydroxynaphthalene (TNH) reductase BRN1 and BRN2, and the scytalone dehydratase SCD1 (Cheung et al., 2020). In our study, the *bcps13* and *bcbnr1* genes are downregulated while the *bcsd1* is up-regulated in  $\Delta$ Bcfrp1. It was reported that deletion of the *bcps13* gene resulted in albino conidia in *B. cinerea* (Zhang et al., 2015), and the *bcbnr1* deletion mutants was deficient in melanin biosynthesis, indicating the disruption of melanogenesis. Meantime, deletion of the *bcsd1* gene mutant also exhibited strong reduction in melanogenesis with no effects on other cellular processes. It was reported that the  $\Delta$ Bcsd1 mutant accumulated scytalone in the culture filtrate rather than the mycelium, and excessive scytalone appears to be self-inhibitory to the fungus (Chen et al., 2021). Therefore, the biological significance of up-regulation of *bcsd1* in  $\Delta$ Bcfrp1 is worth discussing, which may cause the decrease of scytalone accumulation. Some scientists believe that fungal melanin could also be perceived as a molecular pattern of pathogens by their hosts. In ascomycete rice blast fungus *Magnaporthe grisea*, DHN-melanin is a necessary component of the functioning appressorium (Jacobson, 2000). In human-pathogenic fungi *Aspergillus fumigatus*, DHN melanin specifically interferes with functions of host phagocytes, thus ensuring the virulence of the pathogen. Heinekamp et al. (2013) reported that DHN melanin and its precursors, like T4HN, and 1,8-DHN are also able to scavenge host-derived ROS in *A. fumigatus* (Leavitt et al., 2013). In TB-31, the effects of Bcfrp1, Bcpks13, Bcbnr1 and Bcsd1 on pathogenicity remains unclear. Jonkers et al. (2011) observed no effect on pathogenicity when Bcfrp1 in *B. cinerea* B05.10 was targeted for disruption (Jonkers et al., 2011). The *pks13* mutants also did not exhibit any changes in development or pathogenicity, and the effects of BRN1 deletion would be similar to other melanin biosynthesis genes and is nonessential for fungal development and pathogenicity. Therefore, the effect of Bcfrp1 and the functional genes regulated by Bcfrp1 on pathogenicity of *B. cinerea* TB-31 merits further study. In fact, *B. cinerea* TB-31 with substantially increased ABA yields have undergone many rounds of mutagenesis from a wild-type strain TBC-6, which was originally isolated from wheat stem, and leaf (Gong et al., 2014; Ding et al., 2016). Through observation, the mycelial growth of TB-31 is obviously weaker than that of TBC-6, B05.10 and T4, which may affect its colonization on the plant surface (data not shown). Thus, how to design experiments to evaluate the toxicity of TB-31 and  $\Delta$ Bcfrp1 mutant is the next challenge to consider.

Jonkers et al. (2011) compared the growth phenotypes of the  $\Delta$ Frp1 mutants of *F. graminearum*, *F. oxysporum*, and *B. cinerea* on different carbon sources using a Biolog FF assay (Jonkers et al., 2011). The *F. oxysporum*  $\Delta$ Fofrp1 mutant grew significantly less on non-sugar carbon sources, which was very close to the previous growth phenotype on solid plates (Jonkers et al., 2009). In addition, the cell wall degradative genes and isocitrate lyase1 *icl1* were downregulated in the  $\Delta$ Fofrp1 mutant (Jonkers and

Rep, 2009b). On the other hand, the  $\Delta Fgfrp1$  mutant could normally grow on agar plates that contained various non-sugar carbon sources and polysaccharides. The *B. cinerea* B05.10  $\Delta Bcfrp1$  mutants grew well on any carbon source. The 'cross-species' complementation experiment with the *Bcfrp1* of *B. cinerea* to replace the *Fofrp1* of *F. oxysporum*, which led to the growth damage on non-sugar carbon source in  $\Delta Fofrp1$  changed to the growth damage of sugar carbon source in the complementary mutant  $\Delta Fofrp1+$  *Bcfrp1*. Jonkers et al. (2011) postulate that this difference is owing to the promoter sequence of *frp1* (Jonkers et al., 2011). In this study, we compared the colony diameters of TB-31,  $\Delta Bcfrp1$ , and  $\Delta Bcfrp1$ -C on CDA media for 6 days with several carbon sources (Figure 2D). As is shown in Figures 2D,E, after cultivation on CDA medium containing D-glucose and maltose for 6 days, the colony diameter of  $\Delta Bcfrp1$  was significantly reduced to 25, and 37% of that of TB-31, respectively. Moreover,  $\Delta Bcfrp1$  could not grow on CDA plates that contained sucrose. It is obvious that different *frp1* mutants have different phenotypes upon utilizing different carbon sources, which is worthy of further study. We have also considered whether there is such a possibility that *bcrp1* knockout affected the basic metabolism including carbon metabolism, and then indirectly affected the biosynthesis of ABA in TB-31. According to our observation, the different levels of expression of genes involved in the MVA pathway and the ABA biosynthetic gene cluster may lead to ABA deficiency in the  $\Delta Bcfrp1$  strain. But we also found some genes involved in putative sugar transport and degradation, and the gene encoded hexokinase (*Bcglk*), were upregulated. Thus we do not know whether some products of sugar metabolism inhibit the pathway of ABA synthesis. Therefore, it is necessary to expand the screening range of carbon sources, detect ABA yields and the expression patterns of related genes under different carbon sources, and jointly analyses to gain insights into the carbon metabolism and the regulation of ABA synthesis in TB-31 and  $\Delta Bcfrp1$ .

In this research, we found that eight genes were downregulated in the signal transduction pathways, including *bcg1*, *bcras1*, *bcrho3*, *bccdc42*, *bcpka2*, *pzh1*, *bcste20*, and *bc4*. The function of the two genes that encoded serine/threonine-protein kinase *Bcste20* and Calmodulin *Bc4* remains unknown. As reported, the inactivation of *bcg1* (heterotrimeric Gpa2 homolog) caused a decrease in colonies on poor medium with sucrose as carbon source (Gronover et al., 2001), and inactivation by *bcras1* resulted in stunted hyphal growth (Minz Dub et al., 2013). Furthermore, when the *bcras1* gene from another small GTPase family was inactivated, the fungus grew less effectively (An et al., 2015), and the inactivation of *bccdc42* also caused a decrease in hyphal growth (Kokkelink et al., 2011; An et al., 2015). In this study, the *bcg1*, *bcras1*, *bcrho3*, and *bccdc42* genes were downregulated in  $\Delta Bcfrp1$ , which suggests that the decrease in hyphal growth could be related to the decrease in level of expression of these four genes. Fekete et al. (2004) reported that the metabolism of D-galactose except for *via* the Leloir pathway exists as an alternative pathway for hydrolytic D-galactose

metabolism with L-sorbose as an intermediate in *A. nidulans* (Fekete et al., 2004). In this study, the glucose/galactose transporter *gluP* resulted in the downregulation of  $\beta$ -galactosidase, which catalyzes the conversion of lactose to galactose, and  $\alpha$ -galactosidase, which catalyzes the conversion of D-galactose to sorbose, suggesting that the colony diameter of  $\Delta Bcfrp1$  grown on lactose was similar to that of TB-31 and could be related to the alternative pathway of D-galactose metabolism. Ariño et al. (2019) reported that glycogen metabolism and cell cycle control in eukaryotes was regulated by the protein phosphatase PP1 (Ariño et al., 2019). In this study, the genes that encoded protein phosphatase *pzh1* (*glc7* homolog) and the regulatory subunit *Bcglc8* were downregulated, suggesting that downregulation of the genes of glycogen metabolism could be related to the decreased expression of *pzh1* and *bcglc8*. In addition, carbon catabolite repression (CCR) is a global regulatory mechanism that is ubiquitous in microorganisms. In filamentous fungi, CCR is involved in catabolite responsive elements (*CreA*, *CreB*, *CreC*, and *CreD*) as well as the genes of cAMP and Protein Kinase (PKA) signal pathway (Adnan et al., 2017). The mutation of *cre1* in the *fofrp1* deletion mutant restored the impairments in the  $\Delta Fofrp1$  mutant (Jonkers and Rep, 2009b), which indicates that the *Fofrp1* and *Cre1* proteins are both involved in the regulation of the CCR gene in *F. oxysporum*. In this study, we discovered that the regulation of *bccreA* and *bcsnf1* did not change significantly, whereas the expression of *bccreB* and *bccreD* increased in the  $\Delta Bcfrp1$  generated from *B. cinerea* TB-31. Adnan et al. (2017) hypothesized that *CreD* was involved in the ubiquitination of *CreA* and *CreB* was involved in the deubiquitination of *CreA*, respectively (Adnan et al., 2017). The effect of *bccreB* and *bccreD* on the interaction of *bccreA* in *B. cinerea* requires further investigation.

In this study, 30 DEPs with unknown functions were revealed in the signal transduction pathways. We found about 2,661 upregulated DEGs and 1,647 downregulated DEGs, we also found about 627 upregulated DEPs and 446 downregulated DEPs between TB-31 and  $\Delta Bcfrp1$ , suggesting that the changes in the transcription and translation level is very notable. We hypothesize that the effect of *Bcfrp1* on the change of expression level of a large number of genes may be amplified by regulating some signal transduction pathway.

In conclusion, we found that a novel function of *bcrp1* is required for the biosynthesis of ABA in *Botrytis cinerea* TB-31. The deletion of *bcrp1* resulted in the downregulation of the level of expression of the ABA biosynthetic gene cluster and the genes that participate in the mevalonic acid pathway. This study discovered the same regulatory pattern of *Bcfrp1* targeting botrydial (BOT) and bocinic acid (BOA) gene clusters. In addition, DEGs and DEPs participating in the growth and carbon catabolite repression (CCR), and signal transduction in *B. cinerea* were identified based on the transcriptome and proteome data. Our future research will study the DEPs that are regulated by *Bcfrp1* in more detail and search for potential targets in *B. cinerea*.

## Data availability statement

The data presented in the study are deposited in the ScienceDB (<https://www.scidb.cn/detail?dataSetId=bf230977945c4b4785ec355293b23d79>) and accession number (doi: [10.57760/sciencedb.06985](https://doi.org/10.57760/sciencedb.06985)).

## Author contributions

DC contributed to designing and performing the experiments, data analysis, and writing the manuscript. ZW helped with the data analysis. DS and HT helped with revision of the manuscript. All authors contributed to the article and approved the submitted version.

## Funding

This research received financial support from the National Natural Science Foundation of China (32070059). We acknowledge funding from the Technology Innovation Project of Chengdu Science and Technology Bureau (2021-YF05-01197-SN) and Natural Science Foundation of Sichuan (2022NSFSC1634).

## References

- Adnan, M., Zheng, W., Islam, W., Arif, M., Abubakar, Y. S., Wang, Z., et al. (2017). Carbon catabolite repression in filamentous fungi. *Int. J. Mol. Sci.* 19:48. doi: [10.3390/ijms19010048](https://doi.org/10.3390/ijms19010048)
- Alazem, M., and Lin, N.-S. (2017). Antiviral roles of abscisic acid in plants. *Front. Plant Sci.* 8:1760. doi: [10.3389/fpls.2017.01760](https://doi.org/10.3389/fpls.2017.01760)
- Amselem, J., Cuomo, C. A., Van Kan, J. A., Viaud, M., Benito, E. P., Couloux, A., et al. (2011). Genomic analysis of the necrotrophic fungal pathogens *Sclerotinia sclerotiorum* and *Botrytis cinerea*. *PLoS Genet.* 7:E1002230. doi: [10.1371/journal.pgen.1002230](https://doi.org/10.1371/journal.pgen.1002230)
- An, B., Li, B., Qin, G., and Tian, S. (2015). Function of small Gtpase Rho3 in regulating growth, conidiation and virulence of *Botrytis cinerea*. *Fungal Genet. Biol.* 75, 46–55. doi: [10.1016/j.fgb.2015.01.007](https://doi.org/10.1016/j.fgb.2015.01.007)
- Ariño, J., Velázquez, D., and Casamayor, A. (2019). Ser/Thr protein phosphatases in fungi: structure, regulation and function. *Microb. Cell* 6, 217–256. doi: [10.15698/mic2019.05.677](https://doi.org/10.15698/mic2019.05.677)
- Cardozo, T., and Pagano, M. (2004). The Scf ubiquitin ligase: insights into a molecular machine. *Nat. Rev. Mol. Cell Biol.* 5, 739–751. doi: [10.1038/nrm1471](https://doi.org/10.1038/nrm1471)
- Chen, X.-L., Yang, J., and Peng, Y.-L. (2011). Large-scale insertional mutagenesis in *Magnaporthe oryzae* by agrobacterium tumefaciens-mediated transformation. *Methods Mol. Biol.* 722, 213–224. doi: [10.1007/978-1-61779-040-9\\_16](https://doi.org/10.1007/978-1-61779-040-9_16)
- Chen, X., Zhu, C., Na, Y., Ren, D., Zhang, C., He, Y., et al. (2021). Compartmentalization of melanin biosynthetic enzymes contributes to self-defense against intermediate compound scytalone in *Botrytis cinerea*. *MBio* 12, E00007–E00021. doi: [10.1128/mBio.00007-21](https://doi.org/10.1128/mBio.00007-21)
- Cheung, N., Tian, L., Liu, X., and Li, X. (2020). The destructive fungal pathogen *Botrytis cinerea*—insights from genes studied with mutant analysis. *Pathogens* 9:923. doi: [10.3390/pathogens9110923](https://doi.org/10.3390/pathogens9110923)
- Choquer, M., Robin, G., Le Pêcheur, P., Giraud, C., Levis, C., and Viaud, M. (2008). Ku70 or Ku80 deficiencies in the fungus *Botrytis cinerea* facilitate targeting of genes that are hard to knock out in a wild-type context. *FEMS Microbiol. Lett.* 289, 225–232. doi: [10.1111/j.1574-6968.2008.01388.x](https://doi.org/10.1111/j.1574-6968.2008.01388.x)
- Dalmis, B., Schumacher, J., Moraga, J., Le Pêcheur, P., Tudzynski, B., Collado, I. G., et al. (2011). The *Botrytis cinerea* phytotoxin botcinic acid requires two polyketide synthases for production and has a redundant role in virulence with botrydial. *Mol. Plant Pathol.* 12, 564–579. doi: [10.1111/j.1364-3703.2010.00692.x](https://doi.org/10.1111/j.1364-3703.2010.00692.x)
- De Assis, L. J., Ulas, M., Ries, L. N. A., El Ramli, N. A. M., Sarikaya-Bayram, O., Baus, G. H., et al. (2018). Regulation of *Aspergillus nidulans* creA-mediated catabolite repression by the F-box proteins Fbx23 and Fbx47. *MBio* 9, e00840–e00818. doi: [10.1128/mBio.00840-18](https://doi.org/10.1128/mBio.00840-18)
- De Simone, N., Pace, B., Grieco, F., Chimienti, M., Tyibilika, V., Santoro, V., et al. (2020). *Botrytis cinerea* and table grapes: a review of the main physical, chemical, and bio-based control treatments in post-harvest. *Foods* 9:1138. doi: [10.3390/foods9091138](https://doi.org/10.3390/foods9091138)
- Ding, Z. T., Zhang, Z., Luo, D., Zhou, J. Y., Zhong, J., Yang, J., et al. (2015). Gene overexpression and RNA silencing tools for the genetic manipulation of the S-(+)-abscisic acid producing ascomycete *Botrytis cinerea*. *Int. J. Mol. Sci.* 16, 10301–10323. doi: [10.3390/ijms160510301](https://doi.org/10.3390/ijms160510301)
- Ding, Z., Zhang, Z., Zhong, J., Luo, D., Zhou, J., Yang, J., et al. (2016). Comparative transcriptome analysis between an evolved abscisic acid-overproducing mutant *Botrytis cinerea* Tbc-A and its ancestral strain *Botrytis cinerea* Tbc-6. *Sci. Rep.* 6:37487. doi: [10.1038/srep37487](https://doi.org/10.1038/srep37487)
- Dou, T., Wang, J., Liu, Y., Jia, J., Zhou, L., Liu, G., et al. (2022). A combined transcriptomic and proteomic approach to reveal the effect of mogrosin V on ova-induced pulmonary inflammation in mice. *Front. Immunol.* 13:919. doi: [10.3389/fimmu.2022.800143](https://doi.org/10.3389/fimmu.2022.800143)
- Dulermo, T., Rasclé, C., Billon-Grand, G., Gout, E., Bligny, R., and Cotton, P. (2010). Novel insights into mannitol metabolism in the fungal plant pathogen *Botrytis cinerea*. *Biochem. J.* 427, 323–332. doi: [10.1042/BJ20091813](https://doi.org/10.1042/BJ20091813)
- Duyvesteyn, R. G. E., Van Wijk, R., Boer, Y., Rep, M., Cornelissen, B. J. C., and Haring, M. A. (2005). Frp1 is a *Fusarium oxysporum* F-box protein required for pathogenicity on tomato. *Mol. Microbiol.* 57, 1051–1063. doi: [10.1111/j.1365-2958.2005.04751.x](https://doi.org/10.1111/j.1365-2958.2005.04751.x)
- Fang, C., Ye, Z., Gai, T., Lu, K., Dai, F., Lu, C., et al. (2021). Dia-based proteome reveals the involvement of cuticular proteins and lipids in the wing structure construction in the silkworm. *J. Proteome* 238:104155. doi: [10.1016/j.jprot.2021.104155](https://doi.org/10.1016/j.jprot.2021.104155)
- Fekete, E., Karaffa, L., Sándor, E., Bányai, I., Seiboth, B., Gyémánt, G., et al. (2004). The alternative D-Galactose degrading pathway of *Aspergillus nidulans* proceeds via L-sorbose. *Arch. Microbiol.* 181, 35–44. doi: [10.1007/s00203-003-0622-8](https://doi.org/10.1007/s00203-003-0622-8)
- Gabriel, R., Thieme, N., Liu, Q., Li, F., Meyer, L. T., Harth, S., et al. (2021). The F-box protein gene Exo-1 is a target for reverse engineering enzyme hypersecretion in filamentous fungi. *Proc. Natl. Acad. Sci.* 118:E2025689118. doi: [10.1073/pnas.2025689118](https://doi.org/10.1073/pnas.2025689118)
- Gietler, M., Fidler, J., Labudda, M., and Nykiel, M. (2020). Abscisic acid—enemy or savior in the response of cereals to abiotic and biotic stresses? *Int. J. Mol. Sci.* 21:4607. doi: [10.3390/ijms211134607](https://doi.org/10.3390/ijms211134607)
- Gill, A., and Patranabis, S. (2021). Phytohormones as potential anticancer agents. *Int. J. Res. Appl. Sci. Biotechnol.* 8, 37–43. doi: [10.31033/ijrasb.8.3.7](https://doi.org/10.31033/ijrasb.8.3.7)

## Conflict of interest

The authors declare that the research was conducted in the absence of any commercial or financial relationships that could be construed as a potential conflict of interest.

## Publisher's note

All claims expressed in this article are solely those of the authors and do not necessarily represent those of their affiliated organizations, or those of the publisher, the editors and the reviewers. Any product that may be evaluated in this article, or claim that may be made by its manufacturer, is not guaranteed or endorsed by the publisher.

## Supplementary material

The Supplementary material for this article can be found online at: <https://www.frontiersin.org/articles/10.3389/fmicb.2022.1085000/full#supplementary-material>

- Gong, T., Shu, D., Yang, J., Ding, Z. T., and Tan, H. (2014). Sequencing and transcriptional analysis of the biosynthesis gene cluster of abscisic acid-producing *Botrytis cinerea*. *Int. J. Mol. Sci.* 15, 17396–17410. doi: 10.3390/ijms151017396
- Gronover, C. S., Kasulke, D., Tudzynski, P., and Tudzynski, B. (2001). The role of G protein alpha subunits in the infection process of the gray mold fungus *Botrytis cinerea*. *Mol. Plant-Microbe Interact.* 14, 1293–1302. doi: 10.1094/MPMI.2001.14.11.1293
- Heinekamp, T., Thywißen, A., Macheleidt, J., Macheleidt, J., Keller, S., Valiante, V., et al. (2013). *Aspergillus fumigatus* melanins: interference with the host endocytosis pathway and impact on virulence. *Front. Microbiol.* 3:440. doi: 10.3389/fmicb.2012.00440
- Hewage, K. A. H., Yang, J. F., Wang, D., Hao, G. F., Yang, G. F., and Zhu, J. K. (2020). Chemical manipulation of abscisic acid signaling: a new approach to abiotic and biotic stress management in agriculture. *Adv. Sci.* 7:2001265. doi: 10.1002/adv.202001265
- Jacobson, E. S. (2000). Pathogenic roles for fungal melanins. *Clin. Microbiol. Rev.* 13, 708–717. doi: 10.1128/CMR.13.4.708
- Jia, R., Hou, Y., Feng, W., Li, B., and Zhu, J. (2022). Alterations at biochemical, proteomic and transcriptomic levels in liver of tilapia (*Oreochromis niloticus*) under chronic exposure to environmentally relevant level of glyphosate. *Chemosphere* 294:133818. doi: 10.1016/j.chemosphere.2022.133818
- Johnk, B., Bayram, O., Abelman, A., Heinekamp, T., Mattern, D. J., Brakhage, A. A., et al. (2016). Scf ubiquitin ligase F-box protein Fbx15 controls nuclear co-repressor localization, stress response and virulence of the human pathogen *Aspergillus fumigatus*. *PLoS Pathog.* 12:e1005899. doi: 10.1371/journal.ppat.1005899
- Jonkers, W., and Rep, M. (2009a). Lessons from fungal F-Box proteins. *Eukaryot. Cell* 8, 677–695. doi: 10.1128/EC.00386-08
- Jonkers, W., and Rep, M. (2009b). Mutation of Cre1 in *Fusarium oxysporum* reverts the pathogenicity defects of the Frp1 deletion mutant. *Mol. Microbiol.* 74, 1100–1113. doi: 10.1111/j.1365-2958.2009.06922.x
- Jonkers, W., Van Kan, J. A. L., Tijm, P., Lee, Y. W., Tudzynski, P., Rep, M., et al. (2011). The Frp1 F-box gene has different functions in sexuality, pathogenicity and metabolism in three fungal pathogens. *Mol. Plant Pathol.* 12, 548–563. doi: 10.1111/j.1364-3703.2010.00689.x
- Jonkers, W., Rodrigues, C. D. A., and Rep, M. (2009). Impaired colonization and infection of tomato roots by the Deltap1 mutant of *Fusarium oxysporum* correlates with reduced CWDE gene expression. *Mol Plant Microbe Interact.* 22, 507–518. doi: 10.1094/MPMI-22-5-0507
- Kato, A., Kurashima, K., Chae, M., Sawada, S., Hatakeyama, S., Tanaka, S., et al. (2010). Deletion of a novel F-box protein, Mus-10, in *Neurospora crassa* leads to altered mitochondrial morphology, instability of Mtdna and senescence. *Genetics* 185, 1257–1269. doi: 10.1534/genetics.110.117200
- Kim, D., Langmead, B., and Salzberg, S. L. (2015). Hisat: a fast spliced aligner with low memory requirements. *Nat. Methods* 12, 357–360. doi: 10.1038/nmeth.3317
- Kokkelink, L., Minz, A., Al-Masri, M., Giesbert, S., Barakat, R., Sharon, A., et al. (2011). The small Gtpase Bccdc42 affects nuclear division, germination and virulence of the gray mold fungus *Botrytis cinerea*. *Fungal Genet. Biol.* 48, 1012–1019. doi: 10.1016/j.fgb.2011.07.007
- Leavitt, S. D., Fernández-Mendoza, F., Pérez-Ortega, S., Sohrabi, M., Divakar, P. K., Vondrák, J., et al. (2013). Local representation of global diversity in a cosmopolitan lichen-forming fungal species complex (Rhizoplaca, Ascomycota). *J. Biogeogr.* 40, 1792–1806. doi: 10.1111/jbi.12118
- Leyronas, C., Bardin, M., Duffaud, M., and Nicot, P. C. (2015). Compared dynamics of grey mould incidence and genetic characteristics of *Botrytis cinerea* in neighbouring vegetable greenhouses. *J. Plant Pathol.* 97, 439–447. doi: 10.4454/JPP.V97I3.003
- Li, B., and Dewey, C. N. (2011). Rsem: accurate transcript quantification from RNA-Seq data with or without a reference genome. *BMC Bioinform.* 12:323. doi: 10.1186/1471-2105-12-323
- Lievens, L., Pollier, J., Goossens, A., Beyaert, R., and Staal, J. (2017). Abscisic acid as pathogen effector and immune regulator. *Front. Plant Sci.* 8:587. doi: 10.3389/fpls.2017.00587
- Liu, T.-B., Wang, Y., Stukes, S., Chen, Q., Casadevall, A., and Xue, C. (2011). The F-box protein Fbp1 regulates sexual reproduction and virulence in *Cryptococcus neoformans*. *Eukaryot. Cell* 10, 791–802. doi: 10.1128/EC.00004-11
- Long, S., Yang, Y., Shen, C., Wang, Y., Deng, A., Qin, Q., et al. (2020). Metaproteomics characterizes human gut microbiome function in colorectal cancer. *NPJ Biofilms Microbiomes* 6, 1–10. doi: 10.1038/s41522-020-0123-4
- Love, M. I., Huber, W., and Anders, S. (2014). Moderated estimation of fold change and dispersion for RNA-Seq data with DESeq2. *Genome Biol.* 15, 1–21. doi: 10.1186/s13059-014-0550-8
- Marumo, S., Katayama, M., Komori, E., Ozaki, Y., Natsume, M., and Kondo, S. (1982). Microbial production of abscisic acid by *Botrytis cinerea*. *Agric. Biol. Chem.* 46, 1967–1968.
- Masso-Silva, J., Espinosa, V., Liu, T.-B., Wang, Y., Xue, C., and Rivera, A. (2018). The F-box protein Fbp1 shapes the immunogenic potential of *Cryptococcus neoformans*. *MBio* 9, E01828–E01817. doi: 10.1128/mBio.01828-17
- Miesel, L., Greene, J., and Black, T. A. (2003). Genetic strategies for antibacterial drug discovery. *Nat. Rev. Genet.* 4, 442–456. doi: 10.1038/nrg1086
- Minz Dub, A., Kokkelink, L., Tudzynski, B., Tudzynski, P., and Sharon, A. (2013). Involvement of *Botrytis cinerea* small Gtpases Bcras1 and Bcrac in differentiation, virulence, and the cell cycle. *Eukaryot. Cell* 12, 1609–1618. doi: 10.1128/EC.00160-13
- Modi, A., Vai, S., Caramelli, D., and Lari, M. (2021). The Illumina sequencing protocol and the Novaseq 6000 system. *Methods Mol. Biol.* 2242, 15–42. doi: 10.1007/978-1-0716-1099-2\_2
- Nambara, E., and Marion-Poll, A. (2005). Abscisic acid biosynthesis and catabolism. *Annu. Rev. Plant Biol.* 56, 165–185. doi: 10.1146/annurev.plant.56.032604.144046
- Rolland, S., Jobic, C., Fevre, M., and Bruel, C. (2003). Agrobacterium-mediated transformation of *Botrytis cinerea*, simple purification of monokaryotic transformants and rapid conidia-based identification of the transfer-DNA host genomic DNA flanking sequences. *Curr. Genet.* 44, 164–171. doi: 10.1007/s00294-003-0438-8
- Sadat, M., Ullah, M., Bashar, K. K., Hossen, Q. M., Tareq, M., and Islam, M. (2021). Genome-wide identification of F-box proteins in *Macrophomina phaseolina* and comparison with other fungus. *J. Genet. Eng. Biotechnol.* 19, 1–14. doi: 10.1186/s43141-021-00143-0
- Sakthivel, P., Sharma, N., Klahn, P., Gereke, M., and Bruder, D. (2016). Abscisic acid: a phytohormone and mammalian cytokine as novel pharmacological with potential for future development into clinical applications. *Curr. Med. Chem.* 23, 1549–1570. doi: 10.2174/0929867323666160405113129
- Sharma, M., Verma, V., and Bairwa, N. K. (2021). Genetic interaction between Rlm1 and F-box motif encoding gene Saf1 contributes to stress response in *Saccharomyces cerevisiae*. *Genes Environ.* 43, 1–15. doi: 10.1186/s41021-021-00218-x
- Shu, D., Tan, H., Zhou, J., Luo, D., Yang, J., Ding, Z. T., et al. (2018). New sesquiterpene cyclase BcABA3 useful for synthesizing 2Z, 4E- $\alpha$ -ionylidenehexane or abscisic acid, preferably D-abscisic acid, comprises amino acid sequence. CHN Patent No.: CN108753744B. Beijing, China: China National Intellectual Property Administration.
- Siegmund, U., Heller, J., Van Kann, J. A., and Tudzynski, P. (2013). The Naph oxidase complexes in *Botrytis cinerea*: evidence for a close association with the Er and the Tetraspanin Pls1. *PLoS One* 8:E55879. doi: 10.1371/journal.pone.0055879
- Siewers, V., Kokkelink, L., Smedsgaard, J., and Tudzynski, P. (2006). Identification of an abscisic acid gene cluster in the grey mold *Botrytis cinerea*. *Appl. Environ. Microbiol.* 72, 4619–4626. doi: 10.1128/AEM.02919-05
- Siewers, V., Smedsgaard, J., and Tudzynski, P. (2004). The P450 monooxygenase Bcaba1 is essential for abscisic acid biosynthesis in *Botrytis cinerea*. *Appl. Environ. Microbiol.* 70, 3868–3876. doi: 10.1128/AEM.70.7.3868-3876.2004
- Takino, J., Kozaki, T., Sato, Y., Liu, C., Ozaki, T., Minami, A., et al. (2018). Unveiling biosynthesis of the phytohormone abscisic acid in fungi: unprecedented mechanism of core scaffold formation catalyzed by an unusual sesquiterpene synthase. *J. Am. Chem. Soc.* 140, 12392–12395. doi: 10.1021/jacs.8b08925
- Wang, Y., Zhou, J., Zhong, J., Luo, D., Li, Z., Yang, J., et al. (2018). Cys<sub>3</sub>his<sub>2</sub> zinc finger transcription factor Bcaba1 positively regulates abscisic acid production in *Botrytis cinerea*. *Appl. Environ. Microbiol.* 84, e00920–e00918. doi: 10.1128/AEM.00920-18
- Wei, Z., Shu, D., Sun, Q., Chen, D. B., Li, Z. M., Luo, D., et al. (2022). The BcLAE1 is involved in the regulation of ABA biosynthesis in *Botrytis cinerea* TB-31. *Front. Microbiol.* 13:969499. doi: 10.3389/fmicb.2022.969499. PMID: 35992717; PMCID: PMC9386520.
- Willems, A. R., Schwab, M., and Tyers, M. (2004). A hitchhiker's guide to the cullin ubiquitin ligases: Scf and its kin. *BBA-Mol. Cell. Res.* 1695, 133–170. doi: 10.1016/j.bbamcr.2004.09.027
- Wu, T., Fan, C.-L., Han, L.-T., Guo, Y.-B., and Liu, T.-B. (2022). Role of F-box protein Cdc4 in fungal virulence and sexual reproduction of *Cryptococcus neoformans*. *Front. Cell. Infect. Microbiol.* 11:806465. doi: 10.3389/fcimb.2021.806465
- Yu, J. H., Hamari, Z., Han, K. H., Seo, J. A., Reyes-Domínguez, Y., and Scazzocchio, C. (2004). Double-joint Pcr: a Pcr-based molecular tool for gene manipulations in filamentous fungi. *Fungal Genet. Biol.* 41, 973–981. doi: 10.1016/j.fgb.2004.08.001
- Zhang, C., He, Y., Zhu, P., Chen, L., and Xu, L. (2015). Loss of Bcbrn1 and Bcpcp13 in *Botrytis cinerea* not only blocks melanization but also increases vegetative growth and virulence. *Mol. Plant-Microbe Interact.* 28, 1091–1101. doi: 10.1094/MPMI-04-15-0085-R